Liquid Crystals
Publication details, including instructions for authors and subscription information:
http://www.informaworld.com/smpp/title~content=t713926090

Engineering liquid crystals for optimal uses in optical communication systems

J. L. De Bougrenet De La Tocnaye[a]
[a] Optics Department, Ecole Nationale Supérieure des Télécommunications de Bretagne, 29238 Brest Cédex, France

Online publication date: 19 May 2010

To cite this Article De La Tocnaye, J. L. De Bougrenet(2004) 'Engineering liquid crystals for optimal uses in optical communication systems', Liquid Crystals, 31: 2, 241 — 269
To link to this Article: DOI: 10.1080/02678290410001648570
URL: http://dx.doi.org/10.1080/02678290410001648570

LIQUID CRYSTALS, VOL. 31, NO. 2, FEBRUARY 2004, 241–269

Taylor & Francis
Taylor & Francis Group

Engineering liquid crystals for optimal uses in optical communication systems

J. L. DE BOUGRENET DE LA TOCNAYE

Optics Department, Ecole Nationale Supérieure des Télécommunications de Bretagne, CS 83818, 29238 Brest Cédex, France;
e-mail: jl.debougrenet@enst-bretagne.fr

(*Received 22 August 2003; accepted 15 September 2003*)

Liquid crystal technology has become, nowadays, one of the core technologies for implementing optical functions for WDM networks. Their advantage, with respect to other materials, is their unequalled engineering capability which is nowadays decisive in providing more flexible and cost effective systems. First, we briefly review the main driving physical features determining their optical and dynamic behaviour, illustrated through various pure or composite liquid crystal materials. Second, we discuss their suitability for use in some telecommunication requirements. Finally we give examples illustrating the huge variety of their possible effects, in particular when engineered with polymer chains.

1. Introduction

Liquid crystal technology is now a core technology commonly used in optical communications. However, the issue of its suitability in meeting telecommunication constraints has not been addressed from a general materials view-point. This is probably because, in contrast to other generic technologies, liquid crystal technology is not monolithic, due to the huge variety of materials and effects which can be provided, and which is the main source of interest in using them. Furthermore, compared with other soft materials, such as (non-LC) organics, they exhibit relatively strong optical effects over short distances and under low voltages. In addition, they benefit from a better industrial maturity, due to the development of the display industry, e.g. reliability, continuous industrial processes, cost effectiveness, etc. Therefore, our objective here is to review the possible engineering (guided, fibre-confined, free-space, etc.) of such materials to meet the specifications generally required for telecommunication systems within the frame of a wavelength division multiplexing (WDM) network environment.

2. Relevant features of WDM optical networks

Due to their relatively slow switching times (from a few μs to a few tens of ms), liquid crystals and composite liquid crystals are inappropriate for high speed operations such as optical packet switching, but very well suited for most current dense WDM operations (e.g. polarization dispersion compensation, gain flattening, wavelength selection, space routing and switching, etc.) involving high data rate transmission (e.g. 40 Gbit sr^{-1}), requiring a full system reliability and optical transparency [1].

Therefore, the first requirement is to maintain transparency. This means that liquid crystal steady states (physically or electrically obtained) have to be guaranteed. Optical losses can result in a reduction of this transparency. Losses arise from various origins, due to materials (e.g. absorption, scattering, and polarization dependence), optical configurations (e.g. free-space beam division, mode coupling in waveguides and fibres, etc.) [2]. The second requirement is the polarization dependence (measured by the polarization dependent loss, PDL) which depends again on the material considered or the optical configurations. In contrast, the response time depends only on liquid crystal dynamics, related to physical or electrical parameters such as anchoring and alignment forces, electric field, orientation, amplitude and time shapes. In relation to this point, liquid crystals offering a wide range of time response (from tens of ms to a few hundred ns) are available and this feature will be adapted to the considered applications (some of them requiring more or less fast switching times). Temperature dependence is another critical issue with liquid crystals, due to phase transitions which impact optical and dynamic properties. Once again, appropriate liquid crystal engineering, enabling us to bypass this issue and temperature control, is provided in different ways (e.g. material choice or external temperature regulation).

We note that all these requirements are strongly

Liquid Crystals ISSN 0267-8292 print/ISSN 1366-5855 online © 2004 Taylor & Francis Ltd
http://www.tandf.co.uk/journals
DOI: 10.1080/02678290410001648570

related, not only to the liquid crystal choice but to stabilization techniques, optical configurations and electrical addressing schemes. In such a framework, the wide range of liquid crystals and the effects they offer is a powerful tool for closely meeting system requirements. Conditions for such engineering will be discussed here from a material and physical view-point. Some examples will then be given, illustrating how this engineering can be achieved to meet most of the current telecommunication system requirements, rather than giving an exhaustive review of all liquid crystal uses which have become very common nowadays, most of them being reported in the reference list.

3. Liquid crystals: brief history and fundamental driving parameters

The history of liquid crystal begins at the end of the 19th century, with the first observations of the Austrian biologist Reinizer [3] and the works of the German physicist Lehmann [4] emphasising the birefringence of some fluids, and the optical behaviour of phase transitions of compounds such as *para*-azoxyanizol (PAA), which exhibit birefringence variations related to phase transitions (from solid to fluid), according to the variation of temperature variations (figure 1).

Since that time, considerable attention has been paid to this field, and the link between mechanical, optical, and electrical behaviour studied extensively. Basically, liquid crystal properties depend on the interaction of a quadruple set of non-scalar quantities from different physical origins, such as induced mechanical and/or electrical stresses, and intrinsic dielectric anisotropy and elastic restoring force [5]. Respective orientations (figure 2) of these fundamental vectors determine both the liquid crystal optical properties (wavelength dependence, index modulation range, etc.) and its dynamics (response time, steady states, etc.). For example, surface interactions (local and strong with liquid crystal encapsulation within polymer, or global and acting along the bulk with twist formation in a uniform structure) represented by the 4th order tensor σ, are at the origin of some varieties of optical behaviour and response times.

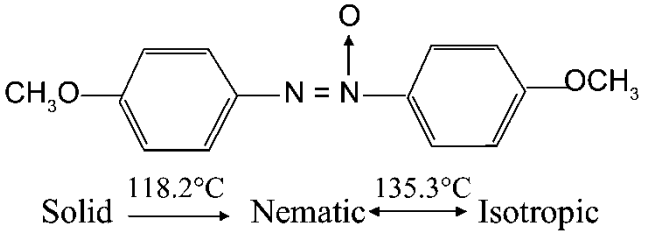

Figure 1. Molecular structure and phase transitions of PAA.

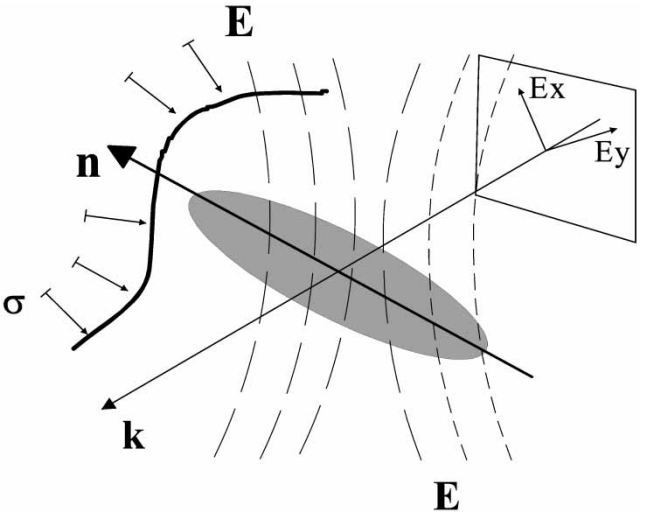

Figure 2. View of interacting quadruple set (**E**, **n**, σ, k), the liquid crystal dielectric anisotropy is represented by the index ellipsoid (in the uni-axial case, the most commonly found), **n** represents the director.

Similarly the orientation, amplitude and time shapes of the applied electric field, competing with elastic (or anchoring) restoring forces, will directly affect the response times. It is the variety of these interactions, which is at the origin of the wide optical and dynamic behaviour of liquid crystals, offering a huge choice of effects, that we propose to present briefly and illustrate by some representative examples of uses.

3.1. *Mechanical stress and flow regime*

Surface interactions impinge on both the dynamic and optical properties of liquid crystals. In contrast to pure crystals, behaviour at interfaces can be different from in the bulk, thus generating a non-uniform structure along the propagation axis, due to larger coherence lengths than for pure crystals. In most practical cases, surface forces are strong enough to impose a well defined orientation to the director **n**. They cause deformations of the director field $\mathbf{n}(r)$, taking into account the elastic forces and the reorientation influence of the external electric field **E**, due to dielectric anisotropy.

Elastic constants and flow regimes determine the restoring torque that arises when the system is perturbed from the equilibrium (by applying an electric field, for instance). It is the balance between the electric torque (forcing molecule reorientation) and the elastic restoring torque that determines the dynamic characteristics. The competing influences on **n** can be expressed by minimizing the free energy density, and LC behaviour explained by the competing effect of

dielectric polarization and elastic deformation on this free energy. Static deformations, illustrated by the distortion stress tensor σ, express the work done when molecules are displaced but each retains its initial orientation. This tensor is not unique and depends on boundary conditions, induced by various surface interactions (e.g. surface anchoring for pure LC or droplet confinement for PDLC) and successive liquid crystal phases. As an illustration, we give the expression of the distortion free energy density in the nematic case for usual deformations (i.e. splay, twist and bend) [6]:

$$F_e = 1/2K_1(\mathrm{div}\,\mathbf{n})^2 + 1/2K_2(\mathbf{n}\cdot\mathrm{curl}\,\mathbf{n})^2 + 1/2K_3(\mathbf{n}\times\mathrm{curl}\,\mathbf{n})^2 \quad (1)$$

where K_1 is the splay constant (for $\mathrm{div}\,\mathbf{n}\neq 0$), K_2 the twist constant for ($\mathbf{n}\cdot\mathrm{curl}\,\mathbf{n}\neq 0$) and K_3 the bend constant (for $\mathbf{n}\times\mathrm{curl}\,\mathbf{n}\neq 0$).

In liquid crystals, another intrinsic characteristic is the flow regime, e.g. viscosity tensor, temperature dependence, etc. These flow regimes are more complex than for pure isotropic liquids, and can be disturbed by a change in alignment, for example by applying an external electric field. From a theoretical view-point, the coupling between orientation and flow is a very delicate matter [7]. An illustration of this coupling may be given in the case of twisted nematics (in the weak twist assumption). Figure 3 displays how the liquid crystal flow can be controlled by an electric field to modulate the incoming light uniformly by appropriate field orientations.

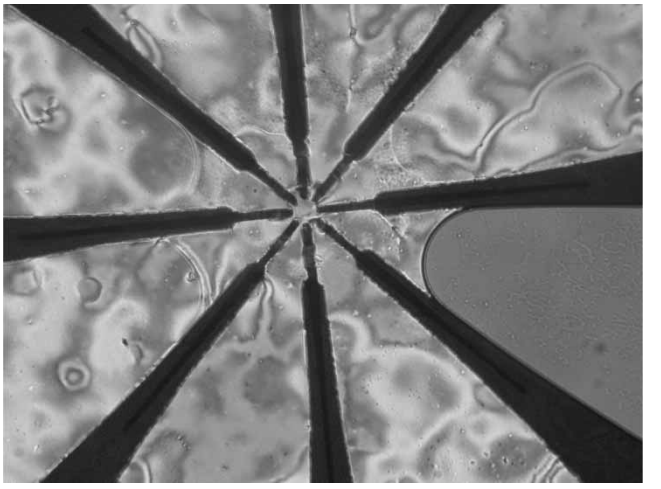

Figure 3. Cross-section of a nematic rotating wave plate [8]. Two distinct regions are observable: the central pupil where the electric field is homogenous thanks to the star-like electrodes, and inter-electrode regions where the liquid crystal flow is free due to relaxed confinement conditions and an inhomogeneous field control.

4. Pure liquid crystal mesophases

The first classification of LC mesophases was proposed in 1920 by Friedel [9]. We only briefly describe here the most commonly used and commercially available phases for which significant technical achievements have been proposed with pure liquid crystals, i.e. nematic (N), twisted nematic (TN) and super-twist (STN), smectic C* and A* (the * means that the molecules are chiral), as well as composites, such as polymer dispersed (PDLC) and polymer stabilized (PSLC) liquid crystals. We mention other effects such as bistable nematics, flexo-electricity, deformed helix and anti-ferroelectricity, for which, up to now, no significant achievements have been made in the telecommunication domain, but could be selected because of meeting some specific system requirements.

Among conventional mesophases, we focus on the two main phases: nematics and smectics (figure 4). The cholesteric phase is illustrated by the twisted nematics, stressing a first distinction between uniform and twisted structures. Another distinction results from the two possible orientations of the director with respect to the electric field and the limiting surfaces: the planar and

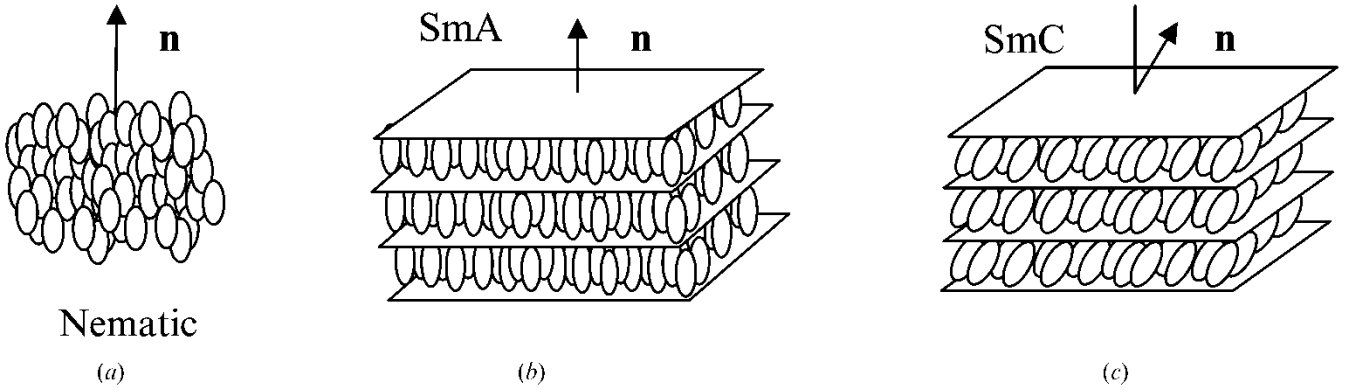

Figure 4. Main liquid crystal mesophases: (*a*) nematic, and homeotropic, (*b*) smectic A and (*c*) smectic C.

homeotropic configurations (figure 5); the latter is relevant only for smectic materials [10]. The planar configuration is the most commonly used, in particular, for display applications. σ is reduced in this case to a vector expressing the surface alignment strength.

4.1. *Uniform nematic liquid crystal*

Only the planar configuration is relevant in this case, the hometropic configuration results in equivalent electro-optical effects. The optical configuration is given figure 5 (*a*). The electric field **E**, the tensor σ (reduced to surface anchoring) and the propagation vector k are collinear, whereas **n** proceeds in the incidence plane. Polarization is induced in this phase by distortions (mechanical or electrical). The application of an electric field **E**, due to a strong dielectric anisotropy ε, results in a dielectric coupling Γ_e expressed by:

$$\Gamma_e = \varepsilon_0 \varepsilon (\mathbf{n}\, x\, \mathbf{E})(\mathbf{n}\cdot\mathbf{E}). \tag{2}$$

If $\varepsilon > 0$, Γ_e tends to align the director **n** in the field direction, whereas if $\varepsilon < 0$, Γ_e tends to align it perpendicular to **E** (figure 6). The optical axis rotation itself induces an index change [11].

When the field is sufficient to overcome the elastic restoring force, the molecules rotate to be collinear with **E** (for a positive dielectric anisotropy). When the electrical field is removed, the molecules relax. Assuming the nematic is uni-axial, the birefringence modulation (in small birefringence approximation) is then expressed as:

$$\Delta n = (n_e - n_o)\cos^2\theta \tag{3}$$

where n_e is the extraordinary index, n_o the ordinary and θ the angle between the optical axis (here the director **n**) and the light propagation direction. In such a configuration the value of the effective index is a function of z and the birefringence defined as:

$$1/n^2(z) = \frac{\cos^2\theta(z)}{n_e^2} + \frac{\sin^2\theta(z)}{n_o^2}$$
$$\Delta n = \frac{1}{d}\int_0^d n(z)\mathrm{d}z - n_0. \tag{4}$$

The response time is proportional to the LC viscosity and inversely proportional to the dielectric anisotropy and the square of the electric field. The major limitation is the intrinsic material elastic relaxation. Typical values of 10–100 ms for thickness $d = 5\,\mu$m are obtained.

The nematic phase has been extensively used because it is easy to manufacture and reliable. A large number of applications have been proposed in the telecommunication domain, including waveguides [12], LPG [13], switches [14], polarization shifters [15], polarization controller [16] and Fabry–Perot tuneable filters [17]). Some illustrations are given and discussed in § 7. The intrinsic absorption of nematics is about $2\,\mathrm{dB\,cm^{-1}}$. This can be a limitation for some waveguide implementations.

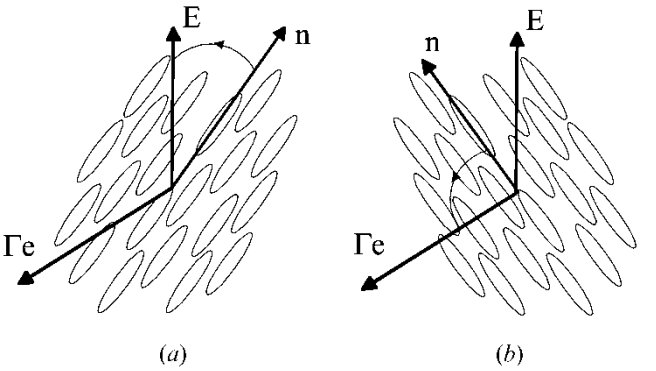

Figure 6. Action of the electric field: (*a*) positive dielectric anisotropy, (*b*) negative dielectric anisotropy.

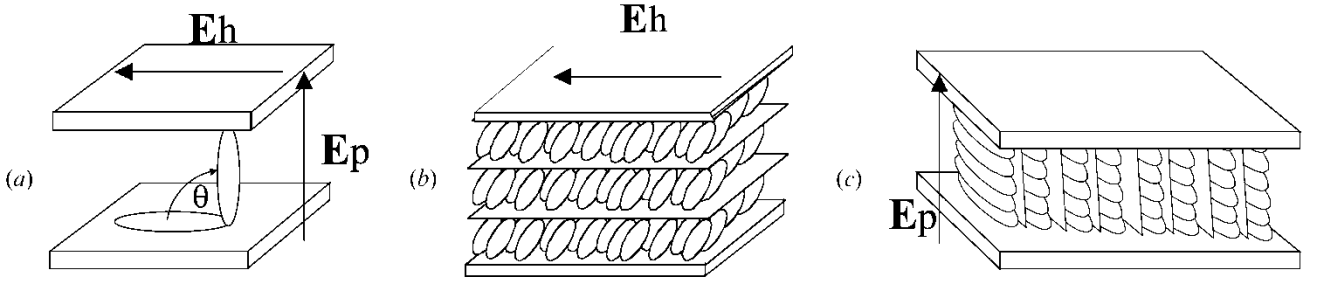

Figure 5. Liquid crystal alignment configurations: (*a*) nematics in planar and homeotropic, (*b*) smectics respectively in the homeotropic (E_h) and (*c*) planar (E_p) configurations.

4.2. *The cholesteric phase*

The helical arrangement is a characteristic of this phase, where the director $\mathbf{n}(r)$ varies in space according to the law:

$$\begin{aligned} n_x &= \cos\theta \\ n_y &= \sin\theta \\ n_z &= 0 \\ \theta &= q_o z + const. \end{aligned} \tag{5}$$

where z is the helical axis and L the helix period equals one-half of the pitch ($L = \pi/|q_0|$). This structure is easily obtained in thin slabs (thickness d in the 100 μm range or less) provided that boundary conditions on both sides of the slab are tangential. Similar effects can be obtained with nematics using a perpendicular surface rubbing (see next section).

4.3. *Twisted nematic (TN)*

In contrast to the uniform case, the glass plates are rubbed following non-parallel orientations (generally perpendicular), thereby inducing a twist as shown in figure 7 (*b*). This is a good illustration of the anchoring force effect along the bulk. When no field is applied to unwind the twist, the material exhibits intrinsic optical activity for polarized light normal to the electrodes, function of Δnd. Assuming the material is divided into incremental slices orthogonal to z [18], when the tilt angle θ is a smoothly varying function of z and voltage V, with even symmetry at the midpoint ($z = d/2$), it is approximated by a mean value only as a function of V. Similarly, if the twist angle is assumed to vary smoothly with odd symmetry at the mid-point, it can be approximated by $\phi = \pi z/d$ and the material can be seen as a combination of optical activity and linear birefringence expressed by following Jones matrix M:

$$M = R(\phi)\begin{pmatrix} \cos X - \mathrm{i}\frac{\Gamma \sin X}{2X} & \phi\frac{\sin X}{X} \\ -\phi\frac{\sin X}{X} & \cos X + \mathrm{i}\frac{\Gamma \sin X}{2X} \end{pmatrix} \tag{6}$$

where $R(\phi)$ is the rotation matrix; Γ the phase retardation in the absence of twist, and X are given by:

$$\Gamma = 2\pi d(n_e - n_0)/\lambda \text{ and } X = \left(\phi^2 + \frac{\Gamma}{2}\right)^{\frac{1}{2}}. \tag{7}$$

In the reflection mode the optical activity is compensated. However, the unwound matrix is difficult to express because it is a function of the voltage. Compared with the uniform case, TNs have larger modulation ranges with respect to the applied voltage, resulting in a better control of the birefringence modulation and a lower sensitivity to thickness variation. In addition, the helix structure has interesting properties (see § 7). Response times are comparable to the uniform case [19]. Extensively used in displays, their main uses in telecommunications concern switching applications [20] for which they provide wide phase modulation ranges.

Observation that electro-optic curves of TN devices were not steep enough to promote multiplexing led Scheffer to develop the first STN display, with higher contrast and modulation range, lower power consumption (due to a smaller switching voltage) than TN but with slower response times (200 ms).

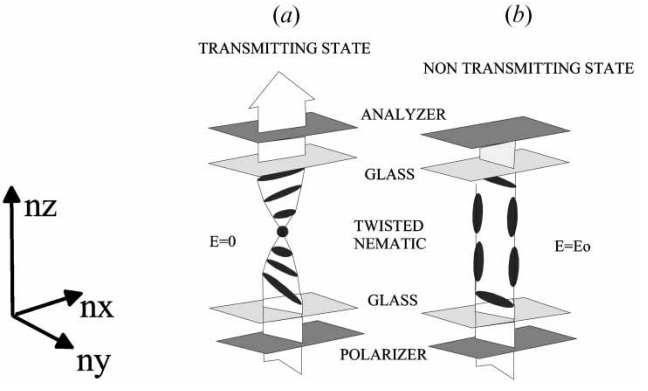

Figure 7. A π twisted nematic, as it is used in display (*a*) in the transmissive state (*b*) in the blocking state.

4.4. *Bistable nematic and twisted nematic*

This is an illustration of strong anchoring effects on LC behaviour [21]. Bistability is due to a mismatch in the nematic natural pitch and cell alignment conditions, for a given thickness. This mismatch is deliberately increased to produce alignment bistability [22]. The resulting advantages are the improved switching speed (due to strong anchoring) [23] and two intrinsic steady states which can be useful for implementing some WDM functions (slowly reconfigurable routers). They are, however, more difficult to manufacture than N or TN materials.

4.5. *Smectic phases*

From a structural view point, smectics are layered structures with a well defined interlayer spacing. They are more ordered and rigid than nematics and less easy to perturb. In contrast to nematics, for which only orientation order exists, they exhibit positional and orientational orders (figure 4), due to the layer structure [24]. There are three main smectic types [6]: smectic A (SmA), smectic C (SmC), and hexatic smectic. We focus here on the more often used SmC* (* means the

molecules are chiral) and SmA. Two configurations must be considered with respect to layer orientation: the planar and homeotropic (figure 5). The natural trend of smectics is to align their layers normal to the limiting surface (i.e. the planar configuration). In the homeotropic case, a layer orientation parallel to the surface is obtained using surfactants such as silane [25]. Lowering the temperature causes the molecules to tilt at an angle θ with respect to the layer normal, forming the SmC phase, the most ordered and least symmetric phase. These two modes exhibit different physical properties that we now describe.

4.5.1. *SmA electroclinic mode (soft mode)*

In this case, it is easy to show that $\mathbf{n}\cdot\mathrm{curl}\,\mathbf{n}=0$, stressing that no twist formation is possible. In addition, a tilt angle θ and a polarization $\mathbf{P}$ are induced when an electric field is applied parallel to the layers, figure 8 (*a*). This electroclinic mode results from the coupling between θ and $\mathbf{P}$ and between $\mathbf{P}$ and $\mathbf{E}$ in the phenomenological Landau free energy expansion [26]. In contrast to the nematic case, the coupling depends on the electric field polarization and a steady state is obtained for $\mathbf{\Omega}=\mathbf{P}=0$, figure 8 (*a*). In the low field regime, this coupling is a linear function and $\mathbf{P}$ is given by:

$$\begin{aligned}&\mathbf{\Omega}=\mathbf{n}\times oz \quad \text{with} \quad \theta=|\Omega|\\ &\mathbf{P}=v\mathbf{\Omega}=v\mu(T)\mathbf{E}\end{aligned} \tag{8}$$

where $\mu(T)$ and v are phenomenological coefficients. The response time is temperature-dependent and its dynamics follow a Lorentzian relaxation law. Typical values, between a few μs and a few 100 ns, gives this mode the fastest liquid crystal electro-optic effect [27]. However, a trade-off has to be found between the speed and the modulation range, related to the tilt angle amplitude [28]. This material exhibits tilt angles as large as $+25^\circ$ but not at submicrosecond speeds. In the homeotropic configuration the material is isotropic in the absence of on electric field, see figure 10 (*f*), later. The main technical limitation of this mode is the field applied perpendicular to the propagation axis which limits its use in displays, but it is well suited for waveguides (see illustration in § 6). Low absorption loss, better than in nematics, makes this material a good candidate for such functions. Other applications include rotating fractional wave-plates [29], Fabry–Perot tuneable filters [30] have been proposed.

4.5.2. *SmC* ferroelectric mode (Goldstone mode)*

We focus on the SmC*, for which a spontaneous polarization $\mathbf{P}_s$ can be observed [24]. Two parameters are needed to describe this mode: $\mathbf{P}_s$ and $\mathbf{n}$, which is a function of the tilt angle θ and the azimuth angle φ (figure 8). However, in this phase in order to observe a macroscopic spontaneous polarization $\mathbf{P}_s$, we must prevent the formation of a natural helix along z. This is done, for example, by using surface stabilization techniques [31] (confinement within a thin cell), which provide another example of strong surface interactions. In this case, due to strong anchoring, only two positions on the smectic cone are possible for $\mathbf{P}_s$, and therefore the orientation of $\mathbf{n}$ depends only on the direction (i.e. the sign) of the electric field $\mathbf{E}$ (figure 8(*b*)). In this case, $\mathbf{E}$, σ and k are collinear with $\mathbf{n}$ perpendicular. Two phases must be distinguished: the ferroelectric and anti-ferroelectric liquid crystal (FLC, AFLC) [25].

4.5.2.1. *Ferroelectric SmC**. In this case the only degree of freedom is the azimuth angle φ. The electro-optic effect is the rotation of the smectic cone driven by coupling between the polarization and external electric field. The coupling energy is

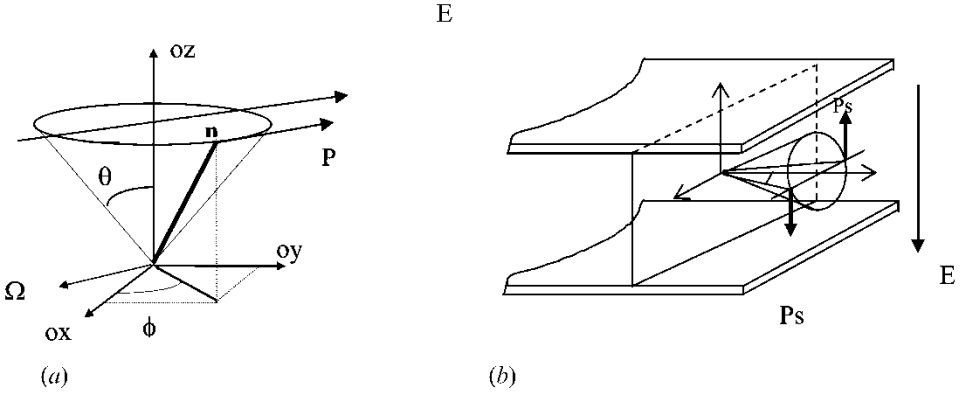

Figure 8. Smectic phases: (*a*) electroclinic SmA, (*b*) SmC*.

$F = -\mathbf{P}.\mathbf{E}$ and an applied field results in an energy variation $-E\delta\mathbf{P}$ from which is derived the expression for ferroelectric coupling:

$$\Gamma = -\left(\frac{\partial F}{\partial \phi}\right) = \mathbf{P}_o \mathbf{E} \sin\phi. \tag{9}$$

Similarly, as in §4.5.1, this electro-optic effect depends on the field polarization. Furthermore, ferroelectric coupling is generally greater than dielectric coupling. This point is at the basis of the fast response time, given by:

$$\tau = \gamma_\varphi / \mathbf{P}_s \mathbf{E} \tag{10}$$

where γ_φ is the smectic phase rotational viscosity. Typical switching times of 10–100 μs are obtained with commercially available materials. This response time is proportional to the rotational viscosity and inversely proportional to the electric field, in contrast to the square relationship for nematics. This results in different electric addressing schemes [32]. In particular d.c. fields must be avoided. Another interesting property is the intrinsic bistability which is, however, difficult to control in practice [33]. Numerous applications have been proposed using FLC materials [34], most concern switching applications [35–37], but include polarization control [38] and waveguides [39].

4.5.2.2. *Anti-ferroelectric SmC and the flexoelectric effect.* In this case, for two adjacent layers, **Ω** and **P** are in opposite directions which results in a macroscopic cancellation of both vectors [40]. Therefore, in conventional uses three different states are accessible: a steady state (AFLC) without field and with field, and two stabilized FLC states depending on the field polarization. Switching times are basically the same as those of a FLC, although relaxation times are slower (about 1 ms).

Other less conventional effects can be found in the literature. Analogue modulation, obtained by a deformed helix ferroelectric liquid crystal [41] or flexoelectricity [42] has been extensively investigated. Flexoelectricity is similar to piezoelectricity in solids; deformation of the LC at the surface generates a polarization which interacts with the electric field [25], resulting in an additional term (F_F) in the distortion free energy relation (1). This is obtained by mechanical forces, an electric field or both (see figure 9):

$$F_F = -e_1(\mathbf{n}\,\mathrm{div}\,\mathbf{n})\cdot\mathbf{E} - e_3(\mathbf{n}\times \mathrm{cur\,ln})\cdot\mathbf{E} \tag{11}$$

where e_1 and e_3 are the flexoelectric coefficients. This results in the observation of a macroscopic polarization. Illustrations of such an interaction are given in figure 9 for weak and opposite anchorings.

Flexoelectricity is important in switching and for a full understanding of induced bistability [43]; however, effects on polarization are in general small (compared with others addressed in this paper), and to our knowledge there are no significant uses in telecommunications. Similarly, the twisted configuration has been investigated with SmC materials [44]. Light is guided in a way similar to that in a twisted nematic; however, a uniform helix is difficult to obtain when operating with a large cell thickness [45], due to the layer structure which trends to align uniformly in the bulk, making the device less attractive than twisted nematics (again there is no significant application in telecommunications to our knowledge).

4.6. *Pure liquid crystal summary*

Nematic liquid crystals are appropriate for applications when a large phase modulation depth is required (2π or greater). They are easy to manufacture, but exhibit low switching times (a few 10 ms). Although new mixtures (e.g. phenyltolane) exhibit high birefringence and faster switching responses (a few ms) they do not operate at room temperature [46]. The issue of the temperature dependence is addressed in §6. With nematics, the reorientation torque is dielectric, whereas with smectics it is due to the electric field polarization coupling. Therefore, smectic materials have good switching times (a few 10 μs), but are more fragile and difficult to manufacture (due to alignment constraints). Typical defects such as chevrons, splay,

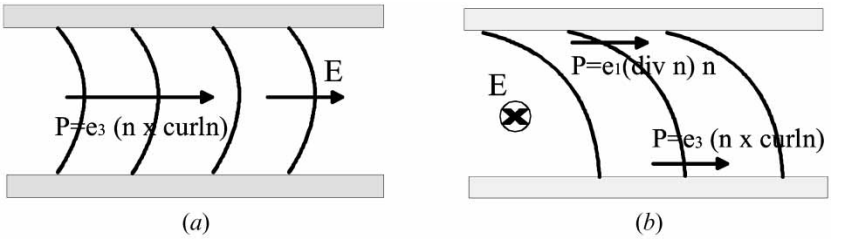

Figure 9. Flexoelectric behaviour: (*a*) under field **E** and for weak anchoring, the directors are bent; (*b*) the director rotates with respect to a perpendicular axis to the cell (torsion) when **E** is applied [43].

etc. are commonly observed with SmC* materials [47], limiting the optical properties. In contrast, SmA materials have no such limitations and exhibit very fast switching times (a few μs and less); in standard mixtures, however, they have a limited modulation range, although new advances, including use of the syloxane chain, have significantly improved this feature [28].

Finally, all liquid crystals require a d.c. balanced drive to prevent damage due to impurities. Because nematics do not respond to the polarity of the applied electric field (positive and negative voltages result in the same optical modulation), an a.c. field can be used, provided a higher frequency than the relaxing frequency is applied. SmC* materials, which respond to the electric field polarization, requires more sophisticated electrical drive schemes or alignment strengths to become transparent. This issue will be addressed in more detail in §6 when dealing with optical transparency. The most commonly used phases and configurations are depicted in figure 10, which illustrates the different variety of effects and uses, for various fundamental quadruple set configurations.

A method of providing better control of liquid crystal dynamics and robustness is to include a polymer chain in the LC molecule, to prevent defect formation and improve the robustness. This has given rise to new optical effects that are described in the next section. Liquid crystals exhibit non-linear also effects [48], such as wave mixing, second harmonic generation, etc. Compared with other organic materials these effects are weaker (due to small second order susceptibility coefficients). However, methyl red doped nematic LCs, and azobenzene LC-doped NLCs have recently been shown to yield non-linear coefficients with orders of magnitude larger than existing materials, and with a response time of a few milliseconds [49]. Nevertheless, we have decided to focus on linear effects, for which liquid crystals are well known to be of greater advantage.

5. Composite liquid crystal materials

Since the pioneering works of Doane [50] and Fergason [51], considerable attention has been paid to LC–polymer mixtures, in particular for

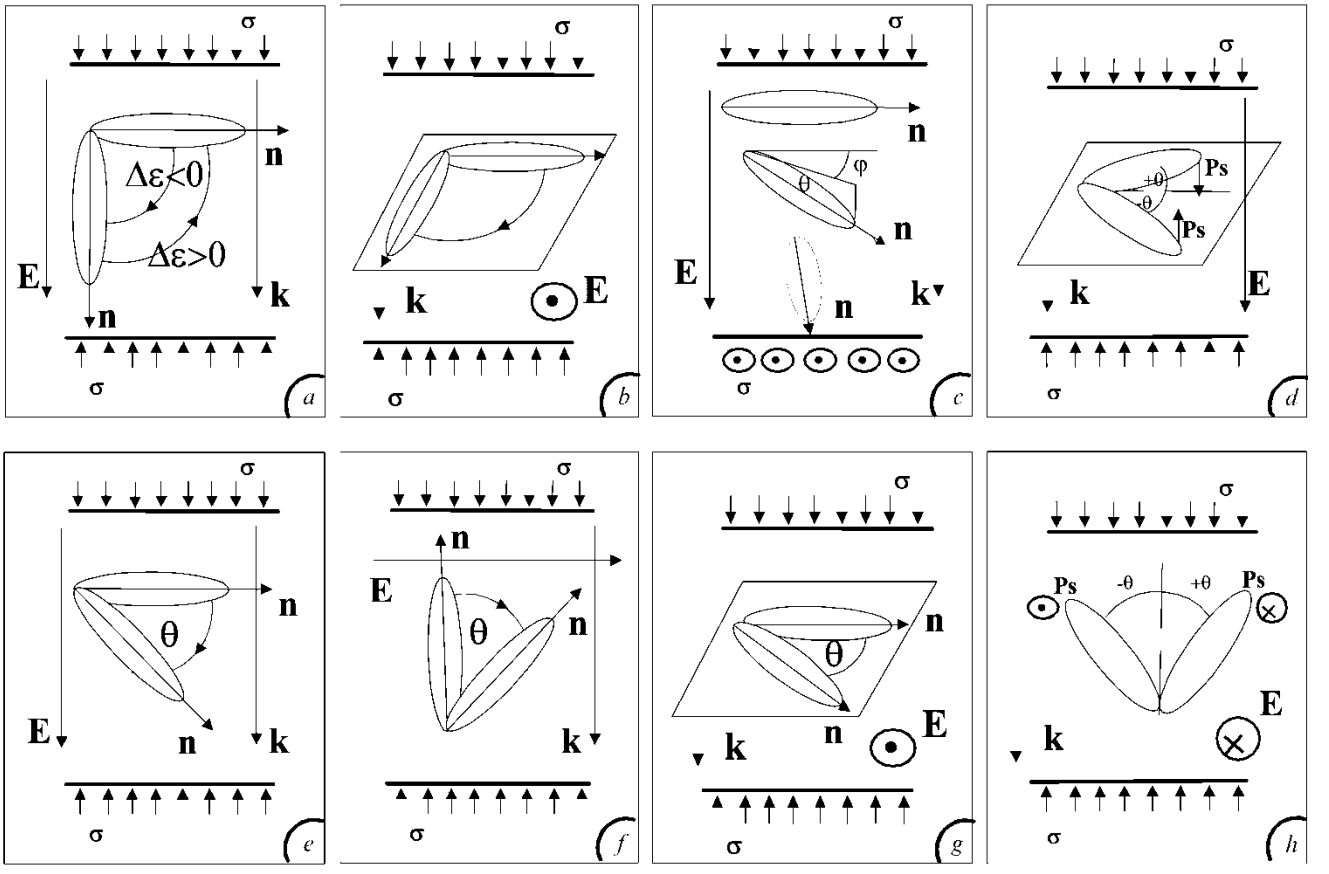

Figure 10. Various quadruple set and LC phases: (*a*) planar and homeotropic nematic, (*b*) planar nematic, (*c*) twisted nematic, (*d*) planar SmC, (*e*) planar SmA, (*f*) homeotropic SmA, (*g*) planar SmA, (*h*) homeotropic SmC.

telecommunications applications. Polymers are added to increase the inherent mechanical strength and/or enhance certain electro-optic properties. Two types of liquid crystal composite mixtures have been designated as polymer dispersed liquid crystals (PDLCs) and polymer stabilized liquid crystals (PSLCs) [52]. PDLCs are characterized by a large percentage of polymer or polymer network (usually $>10\%$) which disperses the liquid crystal into droplets [53]. The properties of such a system are governed largely by surface interactions between the polymer and liquid crystal, and they behave quite differently from pure liquid crystals. PSLCs, on the other hand, have a relatively small amount of polymer ($<10\%$), which is primarily used for stabilization. In these systems the electro-optic behaviour of the LC is not influenced significantly, whereas the mechanical strength is increased dramatically. Most of the PSLC and PDLC systems studied involve nematic or cholesteric liquid crystals, and despite their versatility and potential applications, their usefulness is limited by their relatively slow response times.

5.1. *Polymer dispersed liquid crystal (PDLC)*

The PDLC device comprises a suspension of liquid crystal droplets (generally nematic [50], but possibly chiral [54]) in a host medium (generally a polymer). Liquid crystal director axes within a droplet are determined by the polymer–LC interaction at droplet boundaries (strong anchoring condition) and vary nearly randomly from droplet to droplet in the absence of an applied field. The index mismatch between LC and polymer results in scattering (figure 11) with a constant phase delay. Because the cell thickness is much larger than the droplet size the incident light is scattered many times before emerging from the cell. The degree of scattering and phase delay depend on the size, birefringence and concentration of the droplets.

By controlling the refractive index difference δn between liquid crystal droplets and the host polymer, the PDLC state can vary continuously from opaque to transparent. It is then possible to modulate light by selecting the non-scattered light that passes through the PDLC. When an electric field is applied, LC molecules align along the electric field direction and the material becomes transparent. Liquid crystals with a negative dielectric anisotropy, in homeotropic configuration [51], can also be used. The LC droplets are then aligned parallel to the beam propagation axis in the off-state (no applied voltage), leading to transparency which can be of practical use in some applications. In most PDLCs with micrometer size particles, with a small index discontinuity ($\delta n << 1$) and a droplet size comparable to the wavelength, the scattering cross-section is given, according to Mie scattering theory, by:

$$\sigma = 2\pi\phi^2 \tag{12}$$

and the attenuation related to the scattering cross-section by:

$$I(z) = I(0)\exp(-\sigma N z) \tag{13}$$

where N is the droplet number per unit volume, ϕ the droplet diameter (assuming a spherical geometry) and z

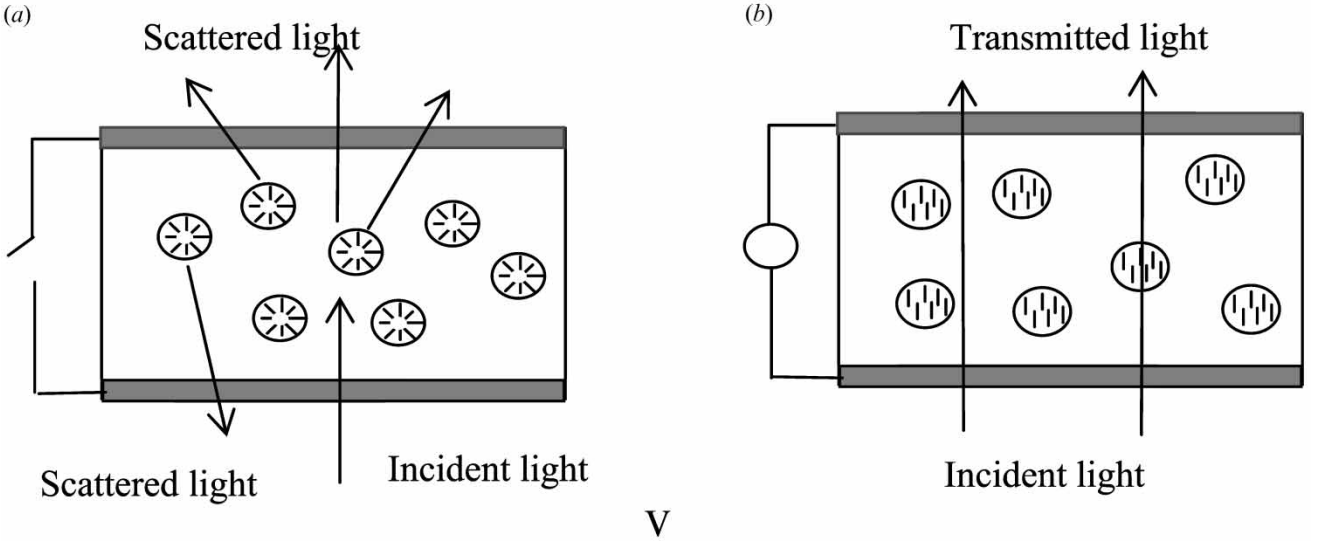

Figure 11. LC droplets are dispersed in a polymer with matching refractive index. (*a*) Scattering occurs in the off-field state ($V=0$) when the liquid crystal molecules are not fully aligned in the droplets. (*b*) LC molecules aligned by applied fied with reduced scattering.

the propagation axis. This relation gives the physical parameters determining the attenuation range. Then for a given droplet size, the higher the liquid crystal concentration (more scatters per unit volume) the better the attenuation dynamics, and the lower the threshold voltage (the concentration is limited only by the LC solubility). Nevertheless, the droplet size must be optimized during the manufacturing process to provide a trade-off between attenuation and low PDL values. The birefringence is fixed by the host polymer to LC compatibility (typical $\Delta n = 0.01$) and the response time is a reverse function of the droplet size (for 1 to 0.5 μm, responses of a few ms are observed), depending, of course, on the liquid crystal. In contrast to pure liquid crystal, there is no intrinsic wavelength dependence (in the C band, the device can be considered as fully achromatic). In addition when used on-axis (light propagating parallel to the applied field), the polarization is inversely proportional to the droplet size (with respect to the wavelength), concentration and birefringence, making the material fully polarization insensitive.

PDLCs have other advantages over pure liquid crystals. Being plastic materials, they need neither polarizer nor surface alignment, unlike liquid crystals. Nevertheless, they keep the same properties of field-induced reorientation of the LC molecules embedded in the polymer matrix. Therefore it is possible to switch the material between two different optical states corresponding to different droplet orientations in the bulk. This gives rise to various applications in telecommunications, mainly to provide low cost high dynamic range variable optical attenuators [56, 57] or dynamic spectral equalizers, when combined with demultiplexing optics [58]. Another interesting capability appears when decreasing the droplet size.

PDLC scattering, being a broad angle phenomenon, must be taken into account in some applications so that undesirable effects such as chromatic dispersion (due to multiple path interferences) and back scattering affecting the extinction ratio can be avoided. Of course the optical set-up is also important. For instance, in conventional 4-f imaging systems, a limited amount of back-scattered light is collected by the imaging optics [58]. Moreover, light scattered at wide angles is not coupled back into the output fibre due to its narrow numerical aperture. In practice, this avoids multiple paths, but possible penalty can result from the attenuation of dynamic range and return loss. However, the directivity and the ratio of back to forward scattering can be engineered by adjusting the scatter size and the liquid crystal birefringence, providing a free parameter to bypass this issue [53].

5.2. *Nano-PDLC and holographic-PDLC*

In the presence of nano-size droplets, transmission is no longer affected when the optical density changes with local droplet density. In this way, for a spatially uniform distribution of droplets, a spatially uniform change in the optical density is obtained with an applied field. Although all liquid crystals can be used, the nematic is preferred because its refractive index varies greatly with orientation change. Various morphologies, obtained by changing size and spatial distribution of the liquid crystal droplets in the polymeric matrix, result in interesting optical effects [52]. For example, a stretched PDLC incorporating uniformly oriented elliptical nematic droplets may serve as a scattering polarizer. However, the most successfully used morphology in telecommunications is the holographic-PDLC (H-PDLC).

5.2.1. *The nano-PDLC principle*

LC droplets with diameters < 150 nm, with respect to telecommunication wavelengths, exhibit faster responses than bulk liquid crystal, and their transmission loss is smaller because they do not function as a scattering medium [59]. The fast response time is related to strong surface anchoring, causing restoring strengths that speed up the LC relaxation time. In contrast, the electro-optic forces needed to switch LC droplets are consequently much higher. As shown in figure 12, without an electric field droplets are randomly oriented. With an applied field along z, LC directors align parallel to **E**, causing the index along z to increase, whereas n_x and n_y decrease. For a propagation vector **k** parallel to **E**, incident light encounters an index variation and the device acts as a pure polarization-insensitive variable phase retarder, whereas birefringence is generated in the yz-plane. Various operations can be achieved by changing the respective orientations of **k** and **E** [60]. When **E** and **k** are collinear, it is possible to estimate the fraction of LC molecules aligned to the field. Let us denote χ_{lc} as the weight fraction of LC in the cell and χ_{al} as the fraction of LC molecules aligned to **E**; it is possible to express the average index as a function of the applied voltage by the following phenomenological expression [59]:

$$\bar{n}(\mathbf{E}) = \chi_{LC}\chi_{al}(\mathbf{E})n_0 + \chi_{LC}[1-\chi_{al}(\mathbf{E})]\bar{n}_{LC} + \chi_{pol}n_{pol} \quad (14)$$

where n_{pol} is the polymer refractive index and n_{LC} the average index of the randomly oriented LC droplets given by:

$$\bar{n}_{LC} = \left(\frac{2n_o^2 + n_e^2}{3}\right)^{1/2}. \quad (15)$$

The average refraction index (for normally incident

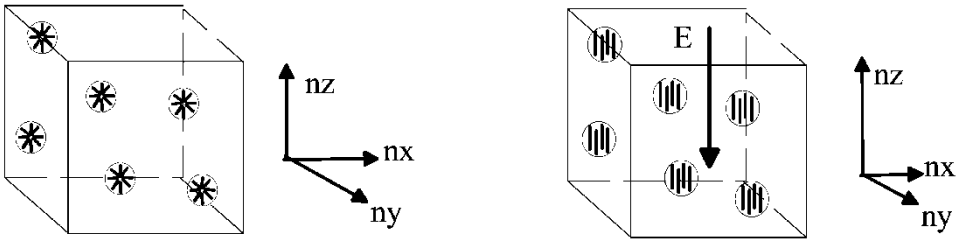

Figure 12. Birefringence and index modulation with nano-PDLC.

light) of the nano-PDLC cell then changes with respect to the voltage by an amount:

$$\Delta\bar{n}_{\mathrm{tot}}(\mathbf{E}) = \chi_{\mathrm{LC}}\chi_{\mathrm{al}}(\mathbf{E})(\bar{n}_{\mathrm{LC}} - n_0). \tag{16}$$

Material investigations have shown that index modulation, for high UV power conditions, as a function of **E**, is given for the weak electrical field approximation by [61]:

$$\Delta n = \alpha \mathbf{E}^2 \tag{17}$$

where **E** is in $\mathrm{V}\,\mu\mathrm{m}^{-1}$ and α is a constant of proportionality depending on the size and density of LC droplets (typically between 10^{-5} and 2×10^{-4} for $n_{\mathrm{e}} = 1.72$ and $n_{\mathrm{o}} = 1.5$ [61]).

For **E** and **k** perpendicular, the material becomes birefringent and the ordinary and extraordinary refractive indices are given by:

$$\begin{aligned} \bar{N}_0 &= x\bar{n}_{\mathrm{o}} + (1-x)n_{\mathrm{polymer}} \quad \text{and} \\ \bar{N}_{\mathrm{e}} &= x\bar{n}_{\mathrm{e}} + (1-x)n_{\mathrm{polymer}}. \end{aligned} \tag{18}$$

In the absence of an electric field, the index is the same as in the first case and is given by equation (10). We notice from equation (11) that a high voltage is required to switch the director (e.g. $30\,\mathrm{V}\,\mu\mathrm{m}^{-1}$). This value is limited by the dielectric breakdown voltage.

Several attempts to reduce voltages have been suggested, for example, by adding plasticizers [62]. More generally, a decrease in droplet diameter reduces the response time but requires higher voltages to compensate the increase in surface boundaries. An increase in droplet diameter decreases voltages, but reduces the speed and introduces losses by scattering. This is the common trade-off of such materials. If nano-PDLC is polarization-independent and exhibits faster response times it requires high voltage values which can limit its use in practice. Steady state switching can occur with ferroelectric PDLC when the droplet size is sufficiently small [63].

Various applications have been proposed using such materials, to implement FP filter arrays [61] (see §7.6.2.), polarization controllers [64], planar waveguides [65], or Mach–Zehnder couplers, by replacing a portion of the waveguide with a nano-PDLC path in one arm or in the cladding. Due to the high voltages, smart addressing, such as for silicon backplane spatial modulators, is difficult to provide. Hence attention has been paid to the fabrication of various shapes and morphologies for nano-PDLCs, and in particular to permanent gratings recorded in the bulk. This technology is based on a new family of composite electro-optic materials called holographic polymer dispersed liquid crystals (H-PDLCs) [66] and electronically switchable Bragg gratings (ESBGs) [67]. Such a nano-PDLC configuration has become one of their main applications, in particular for telecommunication uses [66].

5.2.2. *The holographic PDLC principle*

A homogenous monomer/liquid crystal mixture containing an appropriate photoinitiator is exposed to coherent light to produce an interference pattern inside the material. As the system cures, liquid crystal separates as a distinct phase in the dark fringes of the optical interference pattern. A volume grating is created that consists of periodic PDLC separated by solid polymer [66]. If the film is subject to an electric field, LC molecules reorient with the field (as described in the previous section), changing the optical properties of the hologram. An applied a.c. voltage orients the LC director such that its refractive index matches that of the polymer. The periodic structure vanishes with the electric field, resulting in 0th order diffraction, figure 13 (*a*). Under these conditions a H-PDLC is generally referred to as an electronically switchable Bragg grating (ESBG) [67]. Two main configurations are used: free-space and waveguide. In the first, both transmission and reflection holograms have been exploited, as well as complex elements such as multiplexed holograms. The device behaves as a thick hologram grating, the characteristics of which are given by Kogelnik's coupled wave theory. Polarization dependence and switching response mechanisms have been recently clarified, in the case of un-slanted and un-curved H-PDLC gratings [68] and an extension to

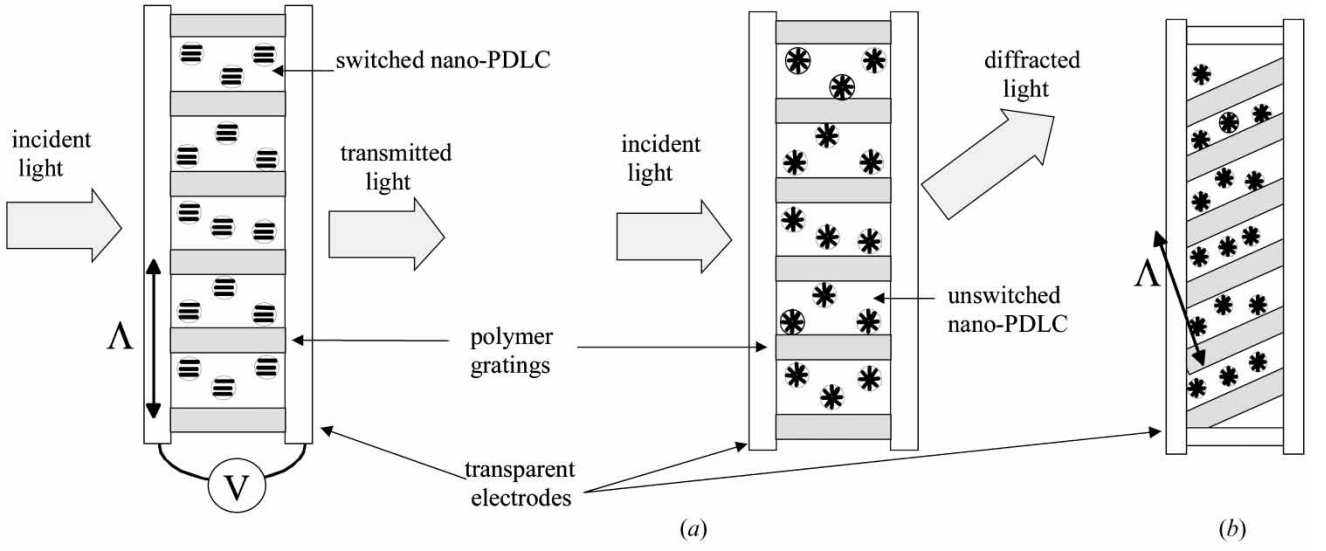

Figure 13. H-PDLC: (*a*) transmission case, (*b*) slanted grating.

subwavelength gratings using H-PDLC has been proposed.

Slanted gratings are preferred for controlling the direction of a diffracted beam, figure 13 (*b*). In a H-PDLC, a slanted grating has various advantages, such as allowing the modulation depth of the grating to be controlled by an electric field when using either planar or homeotropic aligned liquid crystals. This is because the slant provides electric field components in directions both tangential and perpendicular to the grating vector **Λ**. In particular, for the reflection grating the LC domain symmetry axis is oriented along the grating vector and can be switched to a direction perpendicular to the film plane by a longitudinally applied field. This is the typical geometry for switching the maximum diffraction efficiency of a slanted reflection grating.

To obtain high diffraction efficiency and a narrow reflection band it is necessary to optimize the interference pattern regularity of the curing UV radiation to avoid variations in the polymer thickness, as well as obtaining a uniform droplet distribution without broadening the spatial and spectral selectivity. Various techniques have been used to improve these features based, for example, on electromagnetic curing of the LC–monomer mixture [69] or using colloid-templated composites [70]. The addition of surfactants (such as octanoic acids) lowers the switching voltage and improves the diffraction efficiency. This use, combined with a reduction in droplet size, has also been shown to improve switching times (typical values of a few 10 μs have been measured [71]). The surfactant is believed to improve switching voltages by reducing the anchoring forces at the interface between liquid crystal and cured polymer. Various applications have been proposed, including switchable deflectors [72], reflective semitransparent Bragg mirrors, and switchable wavelength filters [73].

Another possible use of ESBGs is their incorporation it into an optical waveguide structure such as the grating, interacting with the mode field outside the waveguide core. An illustration of this principle is depicted in figure 14. In this configuration the waveguide substrate forms one wall of the cell enclosing the nano-PDLC. To exploit LC electro-optic properties, electrodes are deposited onto the walls of the waveguide cell. In use, under an applied voltage, the refractive index of the micro-droplets is reduced, effectively erasing the grating and letting all the light through. With no applied voltage, the grating diffracts

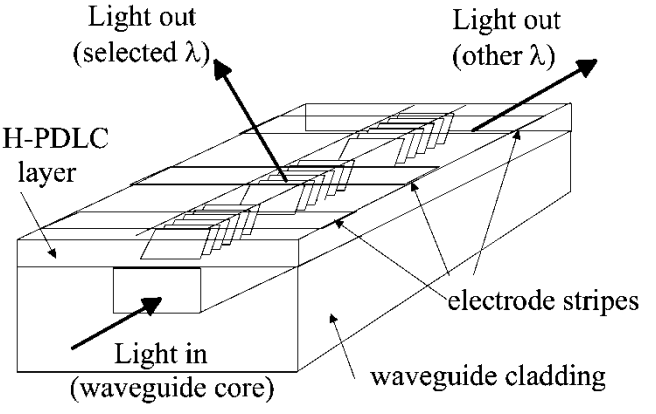

Figure 14. Evanescently coupled electronically switchable Bragg gratings.

light at a specific wavelength out of the waveguide (see principle in § 7.6.1). The advantage of using nano-PDLC instead of pure LC is to avoid polarization dependence due to director-privileged orientations.

Various applications and industrial developments of this technique have been successfully carried out in telecommunications [73], such as variable optical attenuators and wavelength selective filters [67], as well as a planar waveguide Mach–Zehnder 2×2 selective switch [66]. Due to the use of nano-PDLC, ESBG-based devices have good switching speeds ($< 100\,\mu s$), reduced polarization dependence (when an appropriate electrode pattern is implemented) and low power consumption.

5.3. *Polymer stabilized liquid crystal (PSLC)*

The voltage problem of nano-PDLCs or ESBGs (without losing the advantage of strong anchoring) can be bypassed by considering PSLCs which belong to the anisotropic gel family [74], a different system in which liquid crystal alignment is promoted or stabilized by the polymer. They have the same organising property but with lower voltage values [75], due to a relaxed anchoring. Within a PSLC, the LC is stabilized and not encapsulated (figure 15), offering the fundamental advantage of enabling a combination with various liquid crystals, such as a FLC or AFLC [76], which are likely candidates for improving response times up to few orders of magnitude faster than the nematics preferred for their wide phase modulation range. Another advantage of PSLCs is their resistance to mechanical shock, without sacrificing the dynamic properties and behaviours of the liquid crystals they stabilize. Thanks to polymer interaction, the temperature range of the compound, its mechanical properties and switching time are improved [77] and the polymer network prevents the formation of defects. Hence they have been used to improve stability, robustness to shocks and prevention of defects in smectic materials (particularly FLCs and AFLCs), without sacrificing their interesting fast response times.

Another advantage to PSLCs is their extension to chiral LC and cholesteric gels which has opened up a large variety of new electro-optic effects, such as strong optical activity [78] (see § 7.3), as well as the possibility of aligning flexoelectric and FLC films by shearing or stretching, which provides linear bistable and multi-stable effects with switching times down to 20 μs. The response time can be reduced by optimizing the phase separation process.

The application of anisotropic gels to telecommunications is at a very early stage. Up to now they have been mainly used for display applications, such as colour reflective displays [79] (see § 7.3). Their underlying fundamental physics (involving complex relationships between curing conditions, polymer network morphology, interactions between LC and polymer net-work) and their resulting electro-optic properties are far from being fully understood on a quantitative basis. However, they offer a huge potential for applications by broadening the applicability of smectics (already used in telecommunications) to PDLCs, providing new alignment mechanisms, and a myriad of new structural linear and non-linear electro-optic effects in FLC–organic composites. They constitute a full research area. Thick liquid crystal films containing fine polymers have been used, for example, in designing microwave variable phase-shifters with a fast response time [80]. As the liquid crystal alignment becomes unstable in the thick LC film (essential for variable phase shifters), a three-dimensional polymer network is formed in a 100 μm thick LC film to stabilize it. A variable phase-shifter, consisting of a micro-strip transmission line, has been manufactured using the polymer stabilized liquid crystal film as a dielectric material. The device showed a phase shift of 80° at 20 GHz. Attenuation has also be obtained with a PSLC, using the induced scattering effect [81], however,

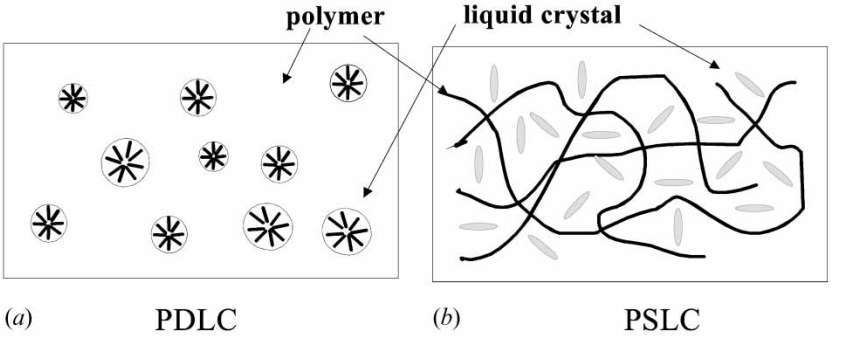

Figure 15. Polymer–liquid crystal composites: (*a*) dispersed, (*b*) stabilized.

the obtained dynamics remain small compared with what can be achieved with conventional PDLCs.

5.4. *Composite liquid crystal summary*

Conventional PDLCs are well suited to provide various types of variable attenuators with decisive advantages, such as polarization and wavelength independence; they provide various material mixings and choices. In contrast, nano-PDLCs are nematic-based. They provide isotropic index modulation but require high voltage, a trade-off for their fast switching speed. The difference between PDLC these forms is related to the droplet size, with respect to the operating wavelength, providing a continuous trade-off between attenuation and phase modulation [59]. H-PDLCs consist of more complex structures which directly affect their response times and polarization dependence. However, they provide a wide range of useful functions for telecommunications, and can be seen as the first attempt to engineer complex polymer–liquid crystal patterns. This will be achieved by PSLCs which are at their early stage of development and applications, and will rapidly find uses in telecommunications due to their robustness and wide range of liquid crystal to polymer combination, shapes and morphologies.

6. Key requirements for telecommunications applications

As with display or military applications, the telecommunications environment imposes particular constraints, some considered as true kill-factors for the applying technologies; most of these constraints are now addressed.

6.1. *Optical transparency*

Various factors can affect optical transparency, e.g. polarization, wavelength dependence, etc. From a system view-point, this feature is commonly assessed with bit error rate (BER) measurements, to guarantee that there are no significant degradations of transmission performance. In the relaxed or steady states, LC and LC composites are transparent materials. Even if orientational director fluctuations or vibrational absorption can occur (resulting mainly in light scattering), such phenomena can be neglected in practice and do not affect transparency, in particular for thin film materials [82]. In contrast, some switching or electrical refreshing regimes can generate transient states or reintroduce time dependence, themselves depending on the liquid crystal nature. As mentioned above, nematics respond to the square of the electric field, whereas smectics respond to the polarity. This makes a major difference, because all liquid crystals require a d.c. balanced drive to prevent damage due to impurities and resulting ion formation. This is easy to achieve with nematics because a.c. voltages can be used, as long as a frequency higher than the relaxing frequency is applied (typically kHz). However, this condition may be more challenging with silicon backplane addressing. With smectics it is not possible and, with some configurations such as SSFLC, a long life time is obtained despite every element spending half of the time in either state. Therefore, the simplest way to achieve d.c. balancing is to switch from one state to its inverse state successively. This can be achieved in display because of the human eye cutting frequency but is absolutely forbidden in telecommunications because interruption of the transmission will result in data loss (the penalty is immediately visible in BER tests).

Three main techniques can be used: the first by inducing strong anchoring, so that physical steady states are obtained. This is difficult to achieve on a silicon backplane and with large tilt angle SmC* materials, due to manufacturing constraints, but has been achieved successfully elsewhere with standard mixtures [30]. The second technique uses a high frequency a.c. field ($>100\,\text{kHz}$) superimposed on the switching pulses. This technique is also used to provide electrical steady states [83], but is difficult to implement on silicon backplane. The third technique, of the software type, is the most appropriate to silicon backplane addressing, in particular for implementing beam steering. A first solution consists in scrolling the optical pattern, generally a grating [84]. In one scrolling step the pattern is translated one pixel width. In this method of d.c. balancing, only a few pixels are switched per scrolling step, so the optical link is kept transparent during scrolling. The device is therefore continuously refreshed. The penalty is a slight reduction of the diffraction efficiency, underlining the need to obtain steady states, not only to guarantee optical transparency but also to reduce the power consumption. This is the case for both FLC and AFLC materials, and for PDLCs with very small droplets. The counterpart is the loss of analogue behaviour due to the presence of two switching states. Therefore, promising solutions are expected with multi stable state PSLCs.

6.2. *Losses*

We now consider losses due to propagation into materials (neglecting multiple reflections between edge windows). They have, of course, various origins and result from different phenomena (absorption, scattering, diffraction, etc.), and are dependent on the optical configuration (thin cell or waveguide). Compared with solids, LC intrinsic absorption and scattering are more

significant, in particular for large cell thickness (a few mm).

A good illustration of such loss (L) mechanisms is given for a nematic cell of thickness d by [85]:

$$L = \left[1 - \left(\frac{n-1}{n+1}\right)^2\right] \exp(-\alpha d) \exp(-\Omega \Phi d) \quad (19)$$

where α is the absorption coefficient, Ω is the scattering loss per unit volume and Φ the cross-section of the incident beam. Strong absorption has several effects on the modulation and electro-optical properties. As a result, order parameter, viscosity, elastic constant and dielectric anisotropy of the LC are modified. In the case of non-linear effects, the absorption-induced thermal lensing effect can compete with the optical field-induced molecular reorientation. Scattering has also to be considered, for large cell thickness. However, in C band, both scattering and absorption are decreasing: scattering as λ^{-4}, and absorption is far off resonances (Ω is about $6.4 \times 10^{-2}\,\mathrm{cm}^{-3}$, in the visible range). Scattering decreases as the temperature increases. Typical absorptions of $20\,\mathrm{dB\,cm}^{-1}$ are observed with standard nematics, about $2\,\mathrm{dB\,cm}^{-1}$ with smectics and $10\,\mathrm{dB\,cm}^{-1}$ with nano-PDLCs (for comparison $0.1\,\mathrm{dB\,cm}^{-1}$ is obtained with organic materials such as polyimide acrylate). In this case, losses mainly due to scattering are related to the droplet size. Of course, in most conventional free-space uses (e.g. thin cells or even thick holograms of a few 10 μm) absorption can be neglected, the device being used as a thin film; such a loss becomes more relevant and can be a real source of limitation for waveguides when the liquid crystal is used as the waveguide core [86] (see § 7.6).

6.3. *Polarization dependence and polarization mode dispersion (PMD)*

Liquid crystals, being anisotropic, act on the polarization. Since the output polarizations of optical transmission systems are unknown and uncontrolled, any LC device must be polarization-insensitive. A good illustration of the effect of this parameter is given by the peak intensity fluctuation of LC Fabry–Perot filters (FPFs), when the polarization input changes [14]. Therefore, except for particular configurations (see § 7.1 and 7.4), polarization diversity systems (PDSs) are generally required, making the system more complex and with possible resulting polarization mode dispersion (PMD). PMD results from the fact that the propagation constants for two eigen-modes become distinct during propagation, for example when circular symmetry of a fibre core is broken by stress or geometrically induced birefringence, or when different path lengths are generated. It is a major impairment for multi-gigabit systems deployment and its effect on direct detection systems through pulse spreading and depolarization causes severe performance degradations.

A conventional PDS combines calcite prisms (or polarized beam splitters) with fixed quarter- or half-wave plates. The principle consists in splitting the input beam (with an incoming unknown polarization) into two orthogonal polarized beams as shown in figure 16, using a calcite prism (a material with linear anisotropy and exhibiting one of the largest split angles). One polarization is then rotated by 90° by a half-wave plate. As a result, the two beams pass trough the LC element with a controlled polarization and are recombined using the reverse principle. When the beams are recombined no interferences occur because they are orthogonally polarized (this means that perfect half-wave plates must be used).

The PDS situations depicted in figures 13 (*a*) and 13 (*b*) are, however, not equivalent with respect to PMD. Different optical paths are generated, due to the double pass into $\lambda/2$ in case (*a*) (in the absence of a compensating plate on the other arm), whereas in case (*b*) the paths have strictly the same length. Optical path balance is a critical PDS issue in preventing PMD. In most cases, PDS is a single input beam splitter (doubling the optical system) with a recombiner at the output, either for an elementary device such as a FPF [14] or for a more complex architecture (see, for example, [87]). But the PDS can also be merged within the optical function itself. A good illustration of this principle has been given with the implementations of 2D switches using polarization shifters [87] implementing various networks schemes [12] such as Banyan or Benès networks. Similarly, the constraint of path

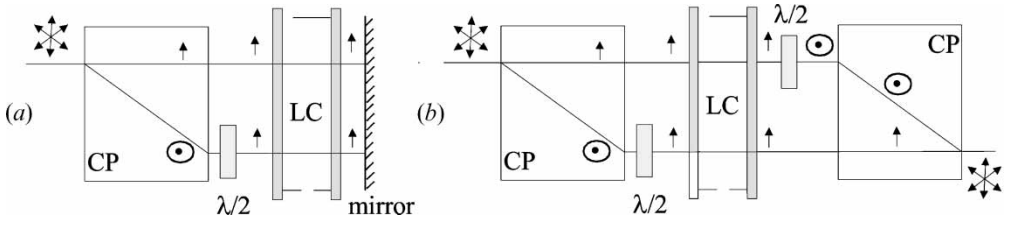

Figure 16. PDS using calcite prisms and half-wave plates: (*a*) used in reflection, (*b*) used in transmission.

balance can be integrated in the network design [88]. Such a combination of fast polarization rotators and calcite beam splitters has given rise to the concept of optical slicer^{TM} as the basis of a range of varied functions [89].

6.4. *Wavelength dependence and chromatic dispersion*

Most applications involving liquid crystals exploit their capabilities easily to modulate either the birefringence (e.g. to implement fractional wave plates), or the refractive index (e.g. to implement phase elements), both parameters that are wavelength-dependent. As stressed by relation (6), fractional wave plates are fundamentally wavelength dependent. In practice, this dependence remains small over the C band and can be neglected in most cases. However, for applications where they are used to switch orthogonal polarization states, or when polarization diversity systems are required, it is necessary to control this parameter to prevent crosstalk or PMD loss.

Except for FLCs, figures 10 (*d*) and 10 (*h*), exhibiting steady states, this can be achieved with LCs by adjusting the voltage to a given λ, assuming only a limited instantaneous bandwidth, e.g. a fraction of the C band (the birefringence modulation being a continuous function of the applied voltage). Wavelength dependence also occurs when implementing pure phase retardation ($\varphi = 2\pi nd/\lambda$), for a given propagation distance d. Wavelength compensation is then achieved by adjusting either d or n (as a function of the applied voltage). Another chromatic dependence occurs when using LCs to implement phase gratings. Because the grating dispersion is more significant for large deviation angles and high diffraction orders, the coupling of grating beam steering functions with fixed location outputs (e.g. a fibre array) can be used to implement wavelength-dependent filters, benefiting from the fine pixel tuning given by liquid crystal grating arrays [90, 91]. An illustration is given in § 7.5 of how wavelength dependence can be used to implement wavelength selectors.

However, wavelength dependence results generally in chromatic dispersion which is a kill factor for high data rate transmission systems. This feature is, however, rarely considered when dealing with LC devices. This dependence is stressed by the presence of intensity ripples, themselves often related to phase ripples due to cavity effects. Such parasitic cavities, caused by interface reflections in optical devices, induce sine-shaped chromatic dispersion [92], making this phenomenon critical. It is, of course, the case for typical Fabry–Perot configurations, but the use of LC or LC composites involves the need for glass substrates, transparent electrodes, alignment layers, mirrors, etc., this requires good index matching between these successive layers and the LC refractive index, with accuracy better than 10^{-2}, to minimize the ripple and chromatic dispersion which can result from the devices itself [53]. In most realizations this point is insufficiently addressed and considered.

6.5. *Response time*

Response times are as varied as liquid crystals themselves, therefore appropriate mixtures can be chosen to control this parameter. Choice of material offers, at room temperature, a range from a few tens ms to a few μs, covering what is generally required for DWDM components, making them good candidates for implementing reconfigurable cost effective functions. From a physical view point, LC response time depends on dielectric anisotropy and improves as its viscosity to elasticity ratio becomes smaller and temperature increases. However, modifying such parameters can affect other characteristics, and is rarely used. In contrast, two properties can improve the switching times: the electric field and the mechanical stress or anchoring forces. A good illustration is given by dual frequency addressing which is a technique devised long ago to improve the response time of some LC displays [93]. At a frequency f_c called the crossover frequency, the dielectric anisotropy, $\Delta\varepsilon = \varepsilon_{\parallel} - \varepsilon_{\perp}$, changes its sign for some mixtures [93]. Therefore, one can electrically alter the optical behaviour of the LC by selecting the driving voltage frequency. In practice $f_c > 1$ MHz and its strong temperature dependence limits its field of application, but it has to be considered when operating over a wide temperature range.

More generally, standard nematics are well known to have slow response times (from a few tens to a few ms) due to slow relaxation, and this value increases with the cell thickness. However, for in-plane switching, figure 10 (*a*), the speed depends upon relative orientations of the electric field with respect to the director. Using star-like electrodes (see § 7.1), and for small rotations of the optical axis, the speed is higher if the initial field is pulsed and directed at a larger angle [88]. Another solution consists in increasing the restoring forces (balancing the intrinsic relaxation). An illustration is given by nano-PDLCs, where anchoring forces balance the relaxation but are offset by the need for more energy to switch the molecules. The disadvantage in both cases is a significant increase in applied voltages. As described in § 5.2.2, the combination of surfactants and a.c. switching voltages at high frequencies can significantly reduce the switching voltages [62].

Another solution consists in driving the liquid crystal with particular electrical schemes. We should mention here that a significant improvement of nematic response times has been obtained using transient effects [94]. The response time of the transition between zero applied voltage and the steady states is greatly reduced when applying a large voltage pulse for short periods of time, before applying the steady state voltage [95]. The main reason for this improvement is the increase in the torque couple applied to molecules during the transition. However, the complexity of LC hydrodynamics makes it difficult to predict quantitatively the conditions required to minimize the response time in the case of spatial light modulators, for which interactions with neighbouring electrodes play a significant role.

In contrast to nematics, smectics exhibit fast switching, three orders of magnitude greater than nematics; SmA are the fastest liquid crystals, although a trade-off has to be found, in this case between operating temperature and tilt angle. The switching times of standard (nematic) PDLCs are similar to nematics; PSLCs reproduce the switching responses of their liquid crystal component [96], making them very attractive when using smectic materials, due to their fast response times and better robustness.

6.6. *Temperature dependence*

The widely accepted reference for specifying environmental behaviour of telecom devices is the Telcordia 1209–1221 recommendations which specify an operating temperature range of $-5/+70^{\circ}$C and a storage range of $-40/+85^{\circ}$C. Liquid crystals are obviously sensitive to temperature change: birefringence and viscosity decrease with temperature increase, and phase transitions appear on increasing the temperature, therefore modifying the material structure. An illustration of such a relationship can be given with nematics. Above the clearing temperature T_c nematics behave as an isotropic liquid, below T_c the long axis tends to align with neighbouring molecules to minimize the total energy and the nematic phase is then observed. The birefringence Δn varies with temperature T, and can be expressed by the empirical approximation [11]:

$$\Delta n \cong g_0 \frac{\lambda^2 \lambda^{*2}}{\lambda^2 - \lambda^{*2}} \exp[-(T - T_0)/T_c] \left(1 - \frac{0.98T}{T_c}\right)^{0.22} \quad (20)$$

where λ^* is the LC resonance wavelength, T_0 the room temperature and g_0 a normalization constant. This indicates why it is necessary to control temperature to maintain the optical and dynamic properties. Military and automotive display applications have long required the manufacture of LC mixtures with broad temperature ranges. For example, nematic ranges can extend from about -20° to 100° [97] but with an effect on transmission characteristics. However, a wide material choice is nowadays available to solve this problem. With composite liquid crystals, the issue is more complicated and depends on the interaction between LC and polymer matrix [97].

Some liquid crystal remains dissolved in the polymer matrix acting as plasticizer, or some uncured polymer precursors remain dissolved in the LC after polymerization, modifying the temperature range and making the combination more complicated. Generally, temperature dependence is smoothed in PDLCs, but the choice of wide temperature range nematics must be made considering their compatibility with a host polymer; in practice this reduces the combinations of materials that can be mixed. Furthermore, in most optical configurations external temperature regulation systems can be accepted, when dealing, for example, with complex functions such as switches, wavelength selectors or dynamic equalizers.

It is also interesting to note that the usual environmental operating temperatures for telecommunication equipment is rarely room temperature, due to proximity to high power sources and highly dissipating electronics. Therefore, it can be a real benefit to select LCs with higher operating temperatures (e.g. 40–50°), then heating them if needed when the overall system is switched off, rather than cooling when the system operates. This is probably another fundamental difference from requirements found in the display industry. Typical examples of such strategies can be found in high power VOA and dynamic gain equalizers using liquid crystals.

6.7. *Resistance to optical power*

Modern optical communications based on the new generation of optical amplifiers often operate with up to 25–30 dB m optical power. The behaviour of all passive devices in the presence of such power, furthermore often focused on small beam spot, can be a critical issue. From this aspect, pure liquid crystals (i.e. without impurities) have the advantage of strong resistance to laser irradiation damage [98]. A first consequence is the change in optical (birefringence) and dynamic (switching time) characteristics, because the LC temperature increases with strong light input. The absorption is converted to heat, with a subsequent warming of the LC molecules. Particular attention has to be paid to the residual absorption and the location of transparent electrodes which are potential heat sources for the material. The solution relies on temperature dissipation and regulation (see §6.6). Such an alteration of the characteristics, due to temperature increase, is partially

smoothed out when using PDLCs. The impact of temperature change is less in case of scattering effects than with pure index or birefringence modulation. This is the reason why such materials are good candidates for high power variable optical attenuators [57].

Another way to overcome this power dependence is to increase the spot size of the input light beam; this becomes particularly significant when using PDLCs due to the increase in scattering centre numbers and then in scattering behaviour.

6.8. *Robustness and power consumption*

Because they belong to the class of soft materials, liquid crystals can be considered as less robust than solids. However, because they can be engineered in several ways, they can benefit from the robustness of the system in which they are embedded (e.g. fibre, wave-guide). The crucial point is irreversible damage in their alignment. In this respect, nematics are more robust than smectics (especially when anchoring is critical such as with SSFLCs), whereas PDLCs are extremely robust due to their polymer host. We recall that the use of a polymer network has been a motivation to make smectics more robust to shock (see § 5.7). Low power consumption is another advantage of LCs due to low voltage requirements and low frequencies needed to switch them. Standard LCs switch with a few $V\,\mu m^{-1}$; composites with strong anchoring constraints such as nano-PDLs and ESBCs require higher voltages (a few $10\,V\,\mu m^{-1}$). In addition when particular electrical schemes with high frequency are required, the overall consumption increases and can be a limitation for some uses in WDM; this is why steady states have been investigated.

Nematics are monostable and an electric field must be continuously applied to maintain the switched states. With conventional nematic PDLCs (i.e. with positive dielectric anisotropy) the transparent state is obtained when an electric field is applied, which means electric field must be maintained when the device does not operate.

A solution consists in using nematics with negative anisotropy (although reducing the choice of polymer/LC mixtures). SSFLCs have the advantage of exhibiting, under certain conditions, two steady states, as also do nano-PDLCs for very small droplet sizes. Once again, PSLCs seem to be the most promising solution for their stabilizing effects.

6.9. *Technology, manufacturing complexity and reliability*

Liquid crystal technology has been commercially applied in LC displays for over 30 years, establishing a proven track record for durability, reliability, performance, and manufacturability. Its recent use in telecommunications has shown that it can meet industry standards for insertion loss, crosstalk, switching speed, path dependent loss, and PDL [99]. Because no moving parts are needed LC performance is stable with respect to temperature change, vibration, and shock. Factors known to accelerate failure in LC devices include UV exposure, high temperature, humidity changes and electrical offsets. With good design, material choice and reasonably controlled exposures, lifetimes of 20 years are expected [100]. Mainly used in thin films, due to their relatively high absorption, evanescent mode coupling in waveguides has been demonstrated successfully. Their fabrication processes are well established, making them the most cost effective technology at present. Compared with pure LCs, PDLCs do not require alignment layers and, similar to PSLCs, various UV curing processes are involved, which makes them more robust.

The combination of various LC compounds opens a wide range of optical effects. In contrast to display requirements, particular attention must to be paid to index matching to avoid cavity effects resulting in chromatic dispersion and PDL. Due to their low voltages, most LCs and LC composites are compatible with silicon backplane addressing, making them appropriate for the silicon industry. LC and LC composite characteristics are summarized in the table.

7. Liquid crystals and composites: some particular uses and refinements

Because of the huge variety of effects and configurations of liquid crystals, their engineering remains a very exciting and innovative field. We propose to illustrate various aspects of this engineering, exploiting different specific optical configurations or LC phases which enable the user to meet the requirements imposed by some basic telecommunication functions.

7.1. *Variable and endless rotating wave plates*

This provides the best example of liquid crystal engineering, exploiting intrinsic structural LC properties (in particular the homeotropic configuration). All types of LCs can be used: nematic [101], electroclinic [102], ferroelectric [103] and nano-PDLC [62]. However, smectics and nano-PDLCs are preferred due to switching times better than conventional nematics. This device is used to provide arbitrary polarization transforms and is critical in implementing optical PMD compensation systems [8]. In free-space, there are three equivalent ways to perform arbitrary polarization transforms. The first uses three wave plates with variable electrically

Table 1. LC and LC composite properties S1 = loss ($dB\,cm^{-1}$), dependence: S2 = polarisation, S3 = temperature, S4 = wavelength, S5 = response time (ms), S6 = modulation range (phase-rd, amplitude-dB), S7 = voltage ($V\,\mu m^{-1}$), S8 = electrical power (W), S9 = robustness, S10 = technical complexity (−weak, + good).

	Property									
	S1	S2	S3	S4	S5	S6	S7	S8[b]	S9	S10
Nematic	20	yes	+	+	50	π	1–2	0.5	−	yes
TN	id.	yes	−	−	50	2π	1	0.5	−	yes
STN	id.	yes	−	−	200	4π	1	0.5	−	yes
BN	id.	yes	+	+	1	< π	10	2.5	−−	yes
SmC*	2	yes/no	−	+	0.1	π	5	2	−−	yes
SmA	2	yes	−−−	+	0.01	< π	5	1	−−	yes
PDLC	10[a]	no	++	−−	30	10−40 dB	2	1	+++	no
Nano-PDLC	10[a]	no	++	−−	0.1	π	10–20	4	+++	no
Holo-PDLC	10[a]	yes	++	+	0.1	π	10–20	4	++	no
PSFLC	2	yes	−	+	0.1	2π	5	2	+	yes

[a]Depends on concentration.
[b]Without temperature regulation.

controllable birefringence and fixed optical axes [38]; the second method uses three wave plates with rotating axes and fixed birefringence [16]; the third combines two variable and rotating wave plates. We focus here on the latter two methods, which provide endless polarization tracking. The materials used are, respectively, SmC* ferroelectric liquid crystal and SmA, both in homeotropic configuration [102]. In the SmA phase birefringence is induced by the electric field, while the SmC* exhibits spontaneous birefringence.

In both cases, polar coupling between the material and the in-plane electric field provides rotating wave plates, with or without phase shift for, respectively, smectic A and smectic C* materials (figure 17).

In a SmA phase, geometrical relations exist between the index ellipsoid principal axis **n** and the electric field **E**, whereas in a SmC* phase, θ is constant and the spontaneous polarization $\mathbf{P}_s$ is parallel to **E**. Therefore, such material can be used to implement two different wave plate types.

7.1.1. *SmC* rotating fractional wave plates*

Three wave plates are required (in sequence quarter, half- and quarter-wave plates) with fixed birefringence, whereas the principal axes can be rotated. A SmC* LC is homeotropically aligned, figure 10 (*d*), and sandwiched between two glass substrates. In this phase, molecules precess on the smectic cone, normal to the electric field direction, figure 14 (*a*), with a fixed angle θ inclined parallel to the substrate. The principal axis depends only on the direction of the applied field. In order to rotate the electric field vector in a plane parallel to the substrates, radial star-like electrodes are etched on the glass substrate (figure 18). Because the cell is thin, it is possible to etch the electrodes on the glass substrate which facilitates complex designs. Retardation is fixed and depends on the field direction, the cell thickness and the birefringence value Δn.

Typical thickness of 20–4 μm in the C band are needed, for quarter- and half-wave plates providing phase shifts close to π. To obtain a large permeation length of **E** within the liquid crystal and a homogenous

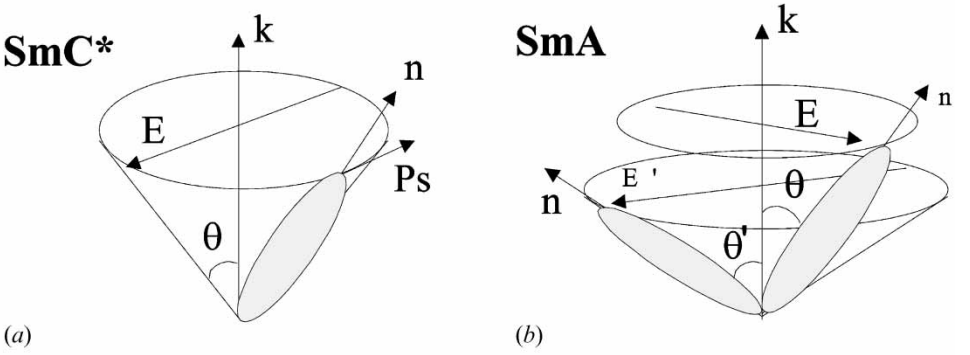

Figure 17. Liquid crystal is uniaxial crystal. Index ellipsoid in geometry of (*a*) SmC* and (*b*) SmA phases.

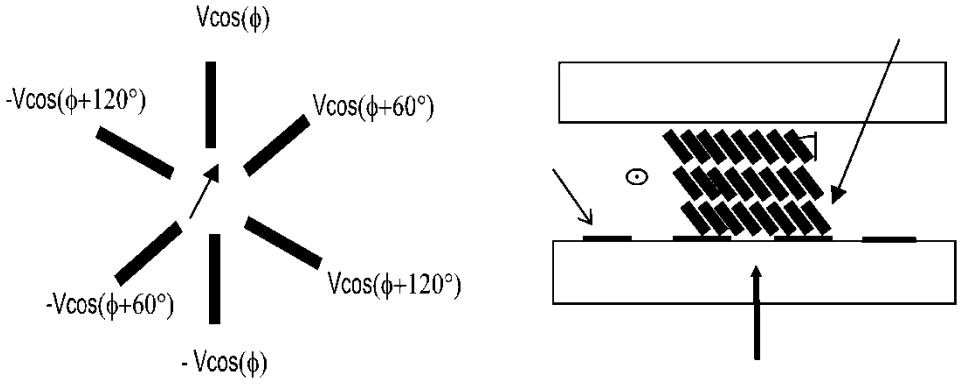

Figure 18. Electrodes implementation on the substrate for a liquid crystal rotating wave plate.

response time, thick electrodes are used (figure 16); typical values $<100\,\mu s$ for $\mathbf{E}=10\,V\,\mu m^{-1}$ at room temperature are commonly observed [103].

The wave plate can also be used in reflection, with the advantages of reduction in thickness and double refraction cancellation. In contrast to nano-PDLCs or nematics (used in the saturation regime), where directors in the bulk are parallel to the glass under an electric field [102], with smectics the directors make an angle θ to the normal which results in double refraction under normal incidence. Double refraction occurs in configurations where both director orientation and inclination are operating, see figures 10 (*c*) and 10 (*d*). Reflective devices enable us to bypass this problem, but require the additional use of a circulator. Another option involves the use of beam coupling into an extended mode fibre (typically 40 μm) [104].

7.1.2. *SmA variable and rotating wave plates*

As with nematics, the variable and rotating wave plate is controlled by two parameters, the applied voltage value and orientation, which drive the rotation on the smectic cone and director inclination, see figure 17 (*b*). Continuous alteration of these parameters produces continuous change in polarization, with a significant gain in control parameters, and then in speed for the monitoring algorithm. A typical phase shift is $\Delta\phi=\pi/2$ for a high electric field value ($10\,V\,\mu m^{-1}$) in C band. This low value of the phase shift (below typical index modulation values of SmA) indicates a decrease of the electric field in the thickness. Therefore, the use of thick electrodes is absolutely necessary in this case. Moreover, the response time is strongly dependent on temperature (1 ms near the SmC*–SmA phase transition and $<100\,\mu s$ near the SmA–I transition). Birefringence modulation can also be used to provide a better control of rotating only the wave plates, making them wavelength adjustable.

In conclusion, liquid crystals present several advantages, such as simplicity, low voltage control, good packaging, no moving parts and no mechanical fatigue; they require, however, careful attention as to alignment over small apertures in the homeotropic configuration (in particular with smectics). Therefore, thick electrodes are recommended to obtain a π phase shift for SmA and homogenous response times for SmC*. In addition, this arrangement avoids residual PDL sources due to the better homogeneity of the applied field and liquid crystal orientation. SmC* materials are well suited to implement fractional rotating wave-plates: they are fast enough, and their birefringence is high and can be slightly adjusted with temperature. Moreover, their optical characteristics remain in the absence of an

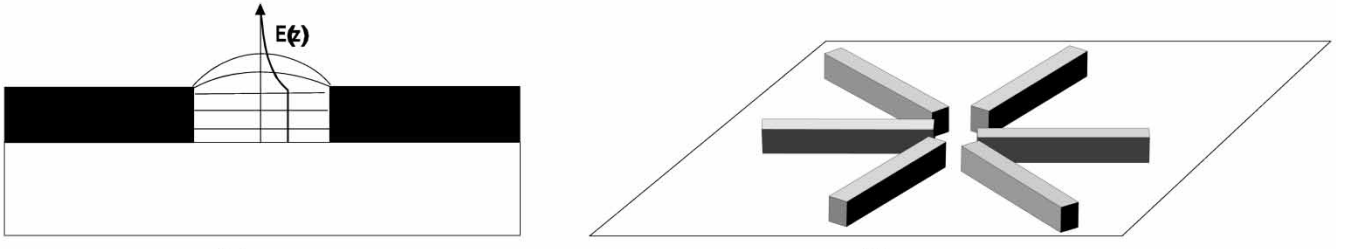

(*a*) (*b*)

Figure 19. (*a*) Transverse electric field with thick electrodes; (*b*) view of thick electrodes system.

applied electric field (steady states on the smectic cone), a feature that can provide a decisive operational advantage. SmAs are well suited to implement variable and rotating wave plates with better speed performance than nematics, despite the temperature control which has to be applied with such materials due to their critical behaviour near transition temperatures. Other solutions have also been proposed using fast nematic liquid crystals [105] or nano-PDLC materials [62]. If both produce better respense times and are easier to manufacture, they do need significantly higher fields ($>20\,\mathrm{V\,\mu m^{-1}}$), resulting in severe optical aperture limitations, making them more difficult to pigtail, collimate and package. Finally, an operational choice cannot only be limited by material aspects, but also by algorithm considerations. Thus variable and rotating wave plates are often preferred, because of the reduction in the number of parameters to control, therefore and simplification of the algorithm.

7.2. *Double refraction-like effects within a ferroelectric SmC waveguide*

Liquid crystals have been extensively used to provide waveguide functions, using various LCs [106, 107] and composite LCs [108]. Most are based on conventional waveguides coupled with active LC claddings [109]. Another less conventional approach involves using the liquid crystal as the guide core [110]. This offers an original illustration of double refraction-like effects. In this framework SmC* is preferred, because it combines good switching time, low absorption ($<2\,\mathrm{dB\,cm^{-1}}$), high birefringence (0.18) and moderate cross-section thickness (a few microns) reducing the insertion and coupling losses. In isotropic media, the beam power flow direction is orthogonal to the wave plane. In anisotropic media it depends on the polarization and the angle β between the index ellipsoid and the wave vector orientations. The extraordinary beam is deflected by an angle φ given by (approximating the beam steering angle in the waveguide):

$$\varphi = \beta - \tan^{-1}\left[\left(\frac{n_e}{n_0}\right)^2 \tan\beta\right] \qquad (21)$$

whereas the ordinary beam has the same direction as the wave vector. In this case the two steady states correspond to two different power flow directions for corresponding extraordinary modes. If these modes are predominant over ordinary modes, a beam steering is observed at the output, accounting for the two double refraction angles. Electrodes can be easily patterned to induce domains of different orientations of the LC director. Collimating integrated lenses are used to control the divergence of the input beam on the yz-plane. Beam shifting can be obtained at the interface of the domains as illustrated in figure 20.

The beams behave in the waveguide plane as in free-space hence they can cross in the same manner. Two types of mode can be excited: ordinary or extraordinary modes. They behave in the planar waveguide as in bulk material. The extraordinary modes, which depend on both the extraordinary and ordinary indices, are deflected at the interface of domains of different orientation of the LC director [9], whereas ordinary modes, which depend only on the ordinary index, are not deflected. An elementary switch can be designed taking advantage of this property. Losses inside the waveguide are due to scattering and absorption which is one of the main drawbacks in using liquid crystals. However, as many switches can be etched on the same guide, there are practically no coupling losses between two adjacent switches. In addition, the LC waveguide is weakly sensitive to wavelength variation ($<10^{-3}$ degrees for 30 nm wavelength deviation, i.e. about a 100 nm lateral shift over 1 cm propagation which is negligible compared with the 150 μm width of a waist beam) [111]. This approach has the advantage of generating equivalent optical paths for all outputs (i.e. equivalent effective index and equivalent length, therefore, preserving the same guided mode), hence there is no PMD. In addition, due to the presence of intrinsic steady states the device can remain switched with no additional power supply due to SSFLC structure.

7.3. *Switchable achromatic reflectors and polarization rotators*

Here we illustrate the engineering offered by polymer stabilized techniques on cholesteric materials. Cholesteric liquid crystals (CLCs) exhibit several remarkable properties due to the presence of a macroscopic helix. The most striking are very large optical activity and

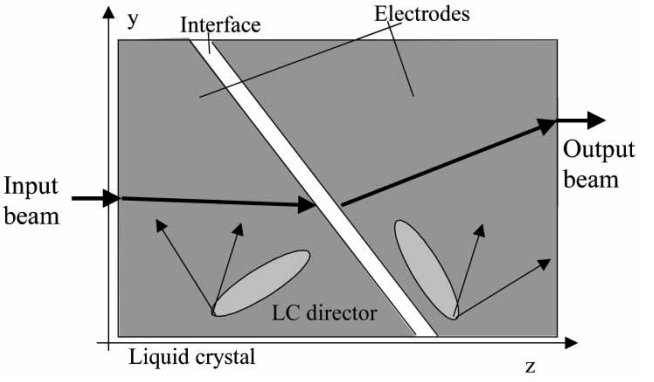

Figure 20. Guide beam refraction at the interface between LC domains of two different orientations.

iridescent colours due to selective reflections displayed by the Grandjean planar texture, when the helix axis is perpendicular to the observation plane [3]. As a result of the helical arrangement of directors, circular birefringence occurs leading to strong optical activity (several thousand degrees per mm). Selective reflection results in spatially periodic variation of the dielectric tensor of the helical structure. For light propagation parallel to the helix, Bragg reflection occurs for wavelengths in the following range (defined as the Bragg regime):

$$n_o p < \lambda < n_e p \tag{22}$$

where p is the CLC pitch (see §4.2). In a small wavelength range around λ_0, incident light parallel to the helix is split into two circularly polarized components: one transmitted, the other totally reflected. The rotation of the reflected circularly polarized light agrees with the screw sense of the helix (figure 21). At normal incidence, maximum reflection occurs when the incident wavelength $\lambda = \lambda_0 = np$, with $n = (n_0 + n_e)/2$ [112]. It is in the region $\Delta\lambda$ of the pitch band that most optical investigations have concentrated, the reflection bandwidth $\Delta\lambda$ being given by $\Delta\lambda = p\Delta n$.

Another interesting case is the Mauguin regime [113]. If the product of the cell thickness d and the birefringence Δn is much larger than the wavelength:

$$\Delta n\, d >> \lambda \tag{23}$$

the eigenmode becomes linearly polarized, determining the wave-guiding limit (the input light is guided by the twist). This property has been extensively used to make twisted nematics wavelength insensitive, which is crucial for colour display applications [21] ($d > 30\,\mu$m is required in the visible range). Achromatic polarization rotators have been proposed following this principle [114]. A rapid calculation shows that the wave-guiding limit is difficult to reach with a TN liquid crystal with a reasonable thickness and Mauguin minima are generally considered [3], with a penalty in the achromatic range. This is, of course, true in the telecommunication band. Choice of selectivity and operating range is desirable for several functions such as optical filters, polarizer-free reflective mirrors and broadband circular polarizers, but a drawback lies in that conventional CLCs have reflection bands that are too narrow to be useful in telecommunications.

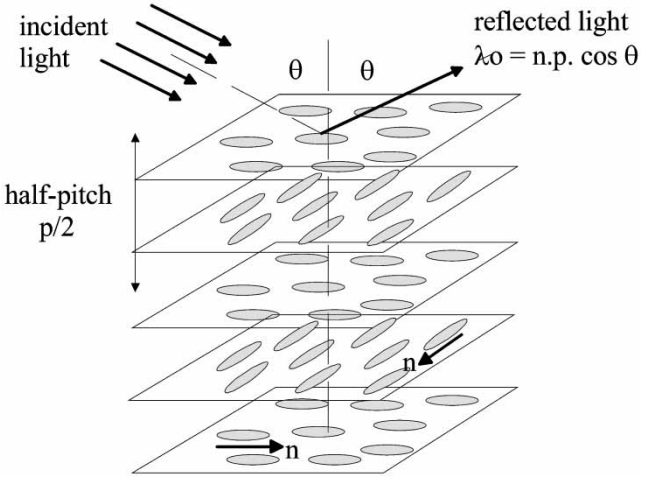

Figure 21. Bragg reflection in a cholesteric helical structure.

Several studies have described broadband CLC filters in the solid state, but only a few have been focused on active filters which are switchable due to the effect of an electric field.

Recent work has shown that some special designs of polymer stabilized cholesteric liquid crystals (PSCLCs) exhibit broadband reflection in the near infrared spectrum on a wavelength band of few hundreds of nanometres greater than expected values in common CLCs [115]. The band broadening results from partial diffusion between two PSCLC films with different chiralities, making them appropriate for telecommunications. This result is a good illustration of the potential offered by PSLC engineering, which is at an early stage.

7.4. *Polarization dependence*

As mentioned in §6.3, liquid crystals, being anisotropic media, are polarization sensitive, and except for some configurations such as those in §7.1 for which anisotropy is needed, polarization diversity systems are required. However, there is a configuration of use for which the LC is purely polarization insensitive. The liquid crystal is used again as a programmable fractional wave plate. The cell is in a planar configuration—i.e. the director rotates in a plane perpendicular to the incident beam, see figures 10 (*a–d*)—and polarization modulation is determined by the birefringence angle $\phi = 2\pi d\Delta n/\lambda$ (with d the cell thickness), the tilt angle θ and the sign $k = +/-1$ of the electric field applied to the cell (figure 22).

The advantage of this configuration is that it leads to a polarization-insensitive phase modulation. Using Jones' formalism ('t' is the transpose operation), an input polarization state $E = [a\ \ b]^t$ expressed in the (C_r, C_l) basis (with C_r and C_l, respectively, the circular right and circular left polarizations) will be transformed by the LC cell in the output state $S(k, \theta, \phi)$

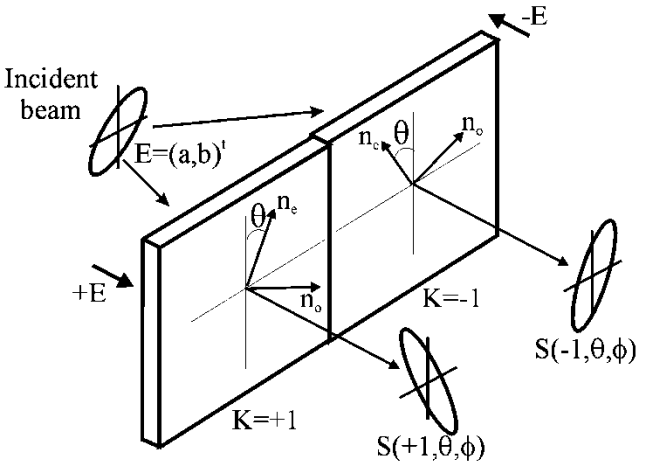

Figure 22. Modulation of the birefringence axes of the LC cell. The normal to the LC layers makes an angle $k\theta$ with the Oy axis of the polarization frame.

given by:

$$S(k,\theta,\phi)=\begin{pmatrix} a\cos\left(\frac{\phi}{2}\right)-ib\sin\left(\frac{\phi}{2}\right)\exp(2ik\theta) \\ -ia\sin\left(\frac{\phi}{2}\right)\exp(-2ik\theta)+b\cos\left(\frac{\phi}{2}\right)\end{pmatrix}. \quad (24)$$

An interesting case is the half-wave plate ($\phi=\pi$) configuration, with $\theta=\pi/4$ tilt angle, yielding

$$S(k,\pi/4,\pi)=k[b-a]^t. \quad (25)$$

Hence, the same polarization emerges from the two LC states, with a π phase-shift between the complex amplitude of the corresponding electric fields [116]. This is a well known use of anisotropic media in optics to achieve polarization-insensitive operations. It has been extensively used, for example, to provide polarization-independent binary phase modulation, avoiding the need for polarization diversity systems [34, 35]. This can be achieved with any planar liquid crystal configuration, provided $\phi=\pi$ (relating to cell thickness) and $\theta=\pi/4$ (relating to the material). Large tilt angle SmC* materials are, however, preferred because they exhibit two intrinsic steady states [10]. The drawback is the wavelength dependence of the wave plate in this configuration; however, this wavelength dependence can be exploited to provide wavelength selectors [90]. A second limitation occurs when using the wave plate as a programmable holographic element due symmetric diffraction orders generated by the binary phase modulation which result in a 3 dB loss. This order can be cancelled by coupling the dynamic LC diffractive grating with an additional fixed phase element [35–91].

The configuration described above is fully justified when using silicon backplane addressing [116], to take a maximum advantage of the available space bandwidth provided by such devices. Such a parallel addressing avoids data transfer bottlenecks (i.e. high speed interfaces similar to MEMS technology), provides very high resolution, an extremely good fill factor, and a large pixel number (see illustration in next section). This combination has been studied extensively to provide a variety of optical free-space switches or filters [34–117].

This principle can be used in a waveguide or fibre configuration. For example, a Mach–Zehnder interferometer (MZI) has been designed on this principle [118], providing a phase shift delay $\Delta\Phi$ between its paths by sandwiching a liquid crystal in the configuration of figure 22. The MZI is made up of two waveguides (or fibres) coupled at their extremities by 3 dB couplers (figure 23); in each MZI arm, a FLC introduces a differential phase shift. Among possible FLC materials, a large tilt angle is needed to verify condition (22) and to enable the optical axis to rotate of 90° on the smectic cone. The two orthogonal states are then addressed by controlling the applied electric field polarization, enabling the routing of the input information to either output 1 or output 2. Both fibre and waveguide can be used to implement such a function. The main crosstalk source is related to wave plate accuracy resulting in technological limitations. To obtain a good isolation (e.g. −30 dB) it is necessary

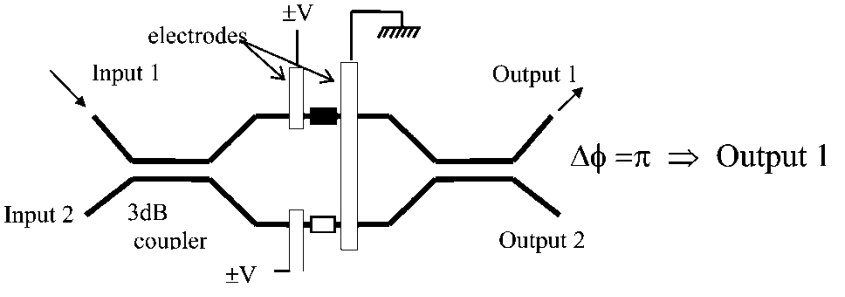

Figure 23. Principle of a FLC MZI: for $\Delta\Phi=\pi$ output 1 is selected; for $\Delta\Phi=0$ output 2 is selected.

to control the cell thickness with an accuracy of 0.3 μm (i.e. for a 4 μm cell, 7% accuracy). This is one reason why nano-PDLC solutions may be preferable.

7.5. *The programmable liquid crystal blazed grating (LCBG)*

Programmable LC blazed gratings are commonly used to implement non-mechanical beam-steering functions [119], thanks to recent advances in LC on silicon backplane technology [116]. Among various diffractive elements, blazed gratings have particularly interesting properties. We focus on linear blazed gratings [120]. Besides a difference in magnitude, blazed gratings combine the dispersive behaviour of a prism (dominated by material dispersion) and of a grating (determined by the diffraction rules). The reverse signs for these dispersions have led to the design of achromatic refractive–diffractive doublets for which the blazed grating is a good illustration. Blazed gratings consist of a series of micro-prisms with constant wedge angles arranged on a periodic grid (figure 24). For a wavelength λ, the maximum height of each prism is fabricated to cause $2\pi q$ phase steps at the prism edges (with q the blaze order). The prism height determines the grating period p, given by:

$$h=\frac{q\lambda}{n-1}, \quad \text{giving} \quad p=\frac{q\lambda}{\alpha(n-1)}. \tag{26}$$

This is equivalent to folding up the phase $2\pi n$ times with respect to λ, which means that the same prism results in two different blazed gratings according to different wavelengths λ and λ' as shown in figure 24. The general equation of a BG calculated for λ' is then given by:

$$\mathrm{BG}=\mathrm{rect}\left[x\frac{\alpha(n(\lambda')-1)}{N\lambda'}\right]\exp\left\{\frac{2\mathrm{i}\pi}{\lambda}\alpha[n(\lambda)-1]x\right\} \otimes\left\{\sum\delta\left[x-\frac{mN\lambda'}{\alpha(n(\lambda')-1)}\right]\mathrm{rect}\left(\frac{x}{p}\right)\right\}. \tag{27}$$

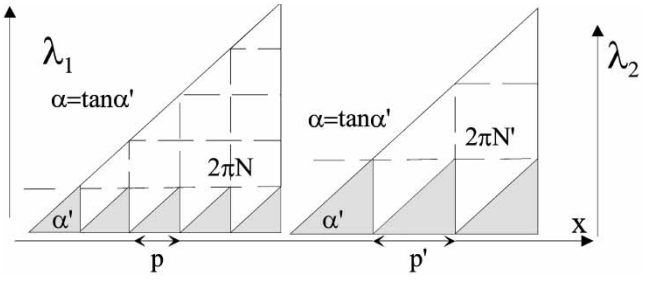

Figure 24. Blazed grating with different blaze depths q as an array of micro-prisms calculated for two different wavelength values ($\lambda 1/\lambda 2=3/5$) and obtained by folding up the phase $2\pi n$ times according to λ.

This expression has two terms (within a convolution product), the first stressing the refractive behaviour of a prism, the second of the grating. The grating behaviour disappears when operating at its generic wavelength λ. This demonstrates that a wavelength adjustment can be achieved by modifying the blaze order q; or by modifying both the period and prism height (here the cell thickness or index amplitude), two parameters of a LC which can be adjusted easily. The result, according to relation (27), is that optimal diffraction efficiency is then obtained because the grating behaves as a prism for the operating wavelength (the generic wavelength has been adjusted to it).

Both uniform and twisted nematics have been used to implement blazed gratings [121]. SmAs can also be used; they are faster but exhibit a smaller modulation range which is a limiting factor for a BG, and remain difficult to implement on LCoS. Therefore, N and TN LCs are preferred. In both cases, polarization diversity systems are required to manage the unknown polarization input state. By applying increasing voltages to successive electrodes (forming a ramp) it is possible to adjust q and generate blaze phase ramps (figure 25). If the gap between electrodes is small enough with respect to the cell thickness, the molecules also rotate in the gap and the phase ramps are quasi-continuous. The phase ramp slope is accurately controlled if each electrode can be supplied with a voltage providing a phase shift $\varphi=2\pi x(\mathrm{mod}\,2\pi)/p$, where x is the lateral position of the electrode and p is the grating period. In practice, the phase retardation has to be greater than 2π, thus a minimum thickness $d=\lambda/\Delta n$ is needed for a cell used in transmission (half for a reflective one), where λ is the operating wavelength and Δn the birefringence.

The drawback is that each electrode has to be addressed independently of the others. This is a challenging issue because the electrode size must be a fraction of the minimum grating period (typically 10 μm). Several techniques developed for LC displays

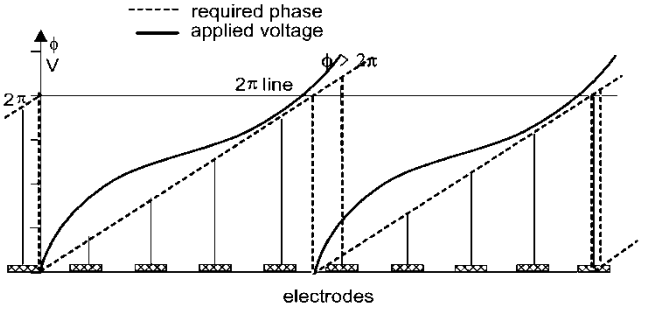

Figure 25. Blazed grating generated by a NLC, with the central fly-back region between two ramps.

are available to solve this problem. For one-dimension electrode arrays, the use of transparent ITO on glass electrodes is a suitable solution. Electrode addressing can be performed by specific integrated circuits bonded at the periphery of the LC cell. An illustration is given in [96] which describes the design of parallel aligned NLC spatial light modulators for operation in the 1.5 μm wavelength range.

For two-dimension electrode arrays, the use of a transparent NLC cell is more difficult: the pixel size achievable with high resolution TFT displays is too large (at least several tens μm). Some miniaturization is thus required. This may be achieved by using LCoS technology, where the active LC electrodes are a silicon integrated circuit. In that case, the device operates in reflection with metal-coated pixels (grating angles are doubled).

The main limitation of this technique is the presence of fly-back regions due to fringing fields between electrodes which diffract into undesired regions, causing crosstalk and reducing the steering efficiency. This phenomenon can be mitigated by adapting the fill factor to the size of the fly-back region (where the phase reset defining a grating period occurs), relatively to the size of the grating period. Another solution involves using a stack of multiple layers of composite blazed gratings of different grating periods. Each layer consists of a fixed blazed grating, obtained and then fulfilled with a liquid crystal. Switching the LC makes the grating transparent or diffracting, but limits the number of addressing steering angles.

LCBG gives a double illustration of the interest in using LC to implement steering functions. First, by exploiting the wavelength independence capability of BGs by only modifying voltage value and period; second, by benefiting from LCoS technology to provide complex volume interconnections. The coupling of liquid crystal with silicon backplane is now the best way to achieve thin film programmable holograms which are strong competitors to MEMs in implementing large capacity switches. The boom of the micro-displays industry has led to commercial high resolution (about 10 μm pitch) devices now reaching 1920×1200 pixels [122] and 2048×1536 pixels with 13.4 μm pitch, with trends towards a decrease in pixel size and an increase in fill factor. If most of the commercial offers are based on twisted nematic liquid crystals, some exist for FLC-based devices with SXGA (1280×1024) resolution [123]. Although these devices operate obviously in the visible wavelength range, no major technical reasons prevent their use in the telecommunications wavelength range.

Despite their larger loss and polarization dependence, the main advantage of liquid crystal holographic modules with respect to, for example, MEMS technology, is their capability to be used not only to steer optical beams but for other purposes such as: the combination of several optical functions (e.g. prism and lens), cross-talk and channel insertion loss reduction (due to fibre misalignments and positioning tolerance), insertion loss uniformity (channel flattening), as well as device fault monitoring, crucial for a large number of output channels. Furthermore, compared with the MEMS approach, they provide natural bridging capabilities, or the spectral response shift of the selected optical output. Some of these advantages are detailed in [119] and [124].

7.6. *Wavelength tuneable filters and lasers*

These devices provide critical functions within WDM networks. We focus on two complementary approaches illustrating particular LC engineering: planar waveguide Bragg grating filters (BGF) and free-space Fabry–Perot interferometers (FPI).

7.6.1. *The Bragg grating filter (BGF)*

This is an alternative to ESBG technique described above (§ 5.2.2). The Bragg grating is written in a planar waveguide and a LC over-layer covers it, acting at the same time as a contrast medium for the filter and as an active cladding for the waveguide (see figure 26) [125].

The Bragg grating etched on the waveguide behaves as a wavelength selective mirror [126] (i.e. a notch filter). Its reflectivity is optimum at the Bragg wavelength λ_B which depends on the physical characteristics of the guiding structure and on the grating geometry and is given by:

$$\lambda_B = 2n_{eff}\Lambda \tag{28}$$

where n_{eff} is the effective refractive index of the guided mode and Λ the grating period. A continuous index variation results in a wavelength change. Therefore, a LC enabling analogue modulation of the extraordinary index, such as N and SmA in a planar configuration, can be chosen. To ensure single mode behaviour, the LC extraordinary index must be smaller than the wave guide. Similarly, transparent electrodes must be thin enough to have negligible effect on the modal behaviour. Experimental results with SmAs have shown

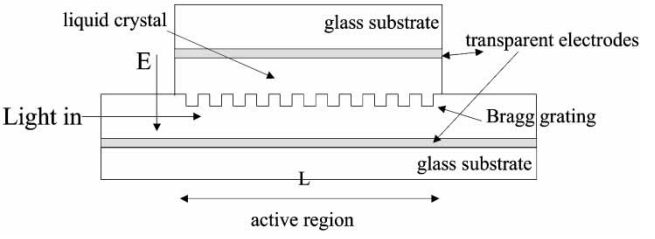

Figure 26. Cross-section of the BGF.

tuning ranges of about 10 nm with good selectivity (<0.5 nm) [127]. Similar operations have been performed with a fibre as guiding medium surrounded by a nematic LC to provide a tuneable long period grating [13] or fibre tapers [128].

7.6.2. *Fabry–Perot interferometer filters and tuneable lasers*

Liquid crystal solutions have been suggested for the implementation of tuneable FPI filters, using nematics [17] and SmAs [30]. The former is too slow, the latter is too fragile and has a smaller modulation range; both are polarization-sensitive, therefore requiring polarization diversity systems (see § 6.3), increasing the cost and introducing additional perturbations and losses. Free-space FPI filters consist of highly reflective parallel dielectric mirrors arranged in a cavity configuration, and separated by a cavity gap L (figure 27). Transparent electrodes allow an electric field to be applied normal to the mirrors and parallel to the propagation axis. The filter transmittance is a function of the phase delay $\varphi = 4\pi nL/\lambda$, and the finesse F (related to mirror reflectivity). For large reflectivity values, F is expressed as the ratio of the free spectral range (FSR) to the filter bandwidth. For wavelength shifts obtained by index change the tuneable range is then given by:

$$d\lambda = 2L\Delta n\Delta\lambda/\lambda. \qquad (29)$$

We notice immediately that nano-PDLCs have a smaller tuneable range than bulk LC, because both Δn (due to concentration) and L (due to voltage limitation) are reduced. Typical $d\lambda$ of a few 10 nm with FSR = 35 nm have been obtained [61], for a typical thickness of about 20 μm, field of 15 V μm^{-1}, switching time of a few 100 μs (two orders of magnitude faster than bulk nematic) and transmission loss <2.5 dB. In practice, to reduce the loss it is preferable to use TEC fibre with expanded modes at the FPI centre to collimate the beam.

Nano-PDLC FPI advantages are polarization-independence, fast switching, low cost and easy fabrication. Its robustness and small size enable it to be combined with arrayed fibres [62]. Similarly, coupling with an active element (in particular with vertical cavity surface-emitting lasers, VCSELs) is straightforward and has been proposed [129]. A 1550 nm VCSEL offers many advantages over edge emitters. They are smaller, cost effective and easy to couple to fibres; they can also be built in matrix arrays. An example of such a coupling is given figure 27 (*b*). The device is a hybrid semiconductor coupled with a nano-PDLC phase layer cavity, surrounded by two dielectric Bragg mirrors. The phase layer optical length is $m\lambda/2 = 6\lambda$ sandwiched between two transparent electrodes appling an electric field with an active region optical length $p\lambda/2 = 1.5\lambda$. The maximum index variation measured with a Mach–Zehnder interferometer is $\Delta n_{max} \approx 0.025$, giving a spectral variation of:

$$d\lambda = \lambda\Delta n/n = (m+p)\Delta\lambda/m \qquad (30)$$

which gives a $\Delta\lambda_{max}$ (for Δn_{max}) of about 20 nm at 1.55 μm.

This is an interesting alternative to the tuneable MEMS VCSEL, using a tuneable source more robust than with MEMS [130]. This solution is easier to manufacture cost effectively, needs no precise mechanical alignments and is more reliable than MEMS. The expected switching time is smaller than for MEMS but the tuning range is also a little reduced. This is a simple

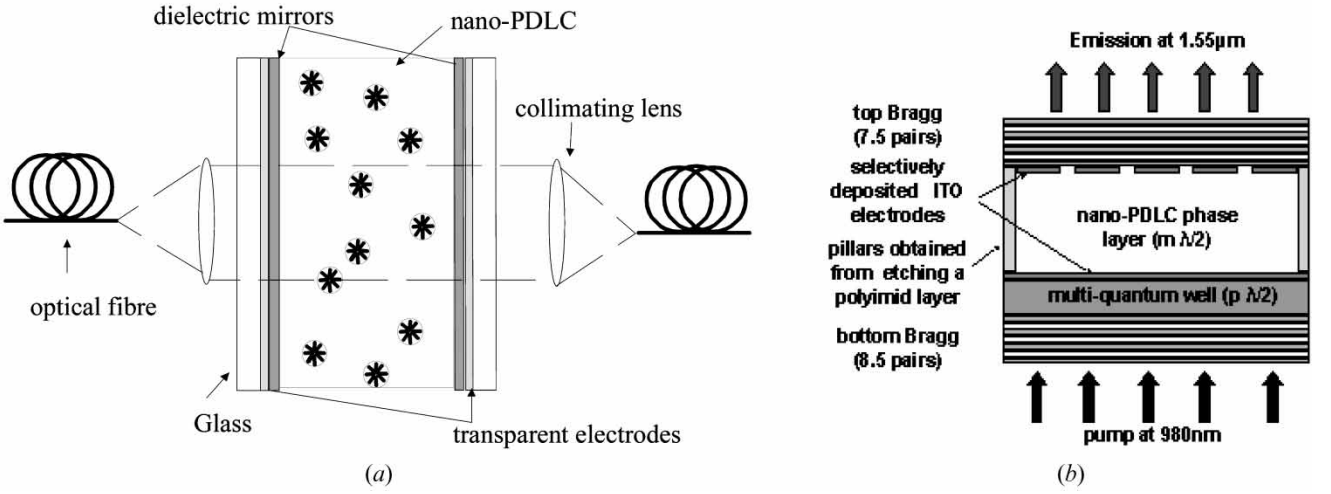

Figure 27. (*a*) Principle of elementary nano-PDLC-based FPI (cross-section); (*b*) coupled with a VCSEL.

illustration of the possible combination of LCs with active elements, which is far from being exhaustive.

8. This is not a conclusion

In the preface to the first edition of his book, P.D. de Gennes stated [6]: *Liquid crystals are beautiful and mysterious, I am fond of them for both reasons. My hope is that some readers of this book will feel the same attraction, help to solve the mysteries and raise new questions*. More fundamentally, their study is complicated by the involvement several scientific disciplines such as, chemistry, optics and mechanics, and also a certain sense of vision in three-dimensional space. If I could modestly add some comments to this analysis, I would say that the applications of LCs in telecommunications are probably at a prehistoric age, and only basic materials have been used till now. The unbelievable recent developments of LC composites and, in particular, anisotropic gels and polymer stabilized LCs, are at an early stage and are endowed with wonderful potentialities, because they enable the use of any LC (cholesteric, nematic, smectic) due to their stabilizing and structuring properties. Therefore, they offer wide possibilities in terms of morphologies, making them very promising in opening a broad field of new effects and functionalities, in particular, for telecommunications which is very demanding in terms of cost and system flexibility. For optical scientists, such materials allow wonderful engineering capabilities which are not fully exploited.

The combination of polymer-curing techniques with the electro-optical characteristics of LCs opens particularly wide prospects, provided a control of particular volume morphologies within the bulk is achieved both to stabilize and generate new optical properties. It is, however, a paradox to notice that photopolymerization is one of the oldest technologies (already used by the ancient Egyptians as part of mummification) which nowadays finds applications in high technology systems. Another recognised advantage of LCs over competitors (such as MEMS) is the strong industrial developments, thanks to the display industry, which provides an unequalled maturity to such solutions, in terms of reliability and cost, making them one of the most appropriate core technologies for DWDM network devices.

The author would like to thank L. Dupont, P. Gautier, P. Gravey, J.R. Brocklehurst and K. Heggarty for fruitful discussions, and for helping him to make this survey more understandable; also successive generations of PhD students who helped him to be convinced that what is written in scientific papers is sometimes true.

References

[1] Borella, M. S., Jue, J. P., Banerjee, D., and Ramamurthy, B. B., 1997, *Proc. IEEE*, **85,** 1274.
[2] Hill, G. R., *et al.,* 1993, *J. Laser Technol.*, **11,** 667.
[3] Reinizer, F., 1889, *Liquid Crystal*, Vol. 5, pp. 421–444.
[4] Lehmann, O. Z., 1889, *Phys. Chem.*, **4,** 462.
[5] Chandresakar, S., 1992, *Liquid Crystals* (Cambridge University Press).
[6] De Gennes, P. G., and Prost, J., 1994, *The Physics of Liquid Crystals* (Oxford University Press).
[7] Leslie, F., 1969, *Mol. Cryst. liq. Cryst.*, **7,** 407.
[8] Dupont, L., de Bougrenet de La Tocnaye, J. L., Gadonna, M., and Sansoni, T., 2003, *Ann. Telecommun.*, **58,** 1.
[9] Friedel, G., 1922, *Ann. Phys.*, **18,** 273.
[10] Clark, N. A., and Lagerwall, S., 1980, *Liquid Crystals of One or Two Dimensional Order* (Berlin: Springer Verlag), pp. 222–236.
[11] Wu, S. T., 1995, *Handbook of Optics* (McGraw Hill), Chap. 14.
[12] Whinnery, J. R., Hu, C., and Kwon, Y. S., 1977, *IEEE JQE*, Vol.13, pp. 262–267.
[13] Duhem, O., Henninot, J. F., Warenghem, M., and Douay, M., 1998, *Appl. Opt.*, **31,** 7223.
[14] Noguchi, K., and Kawakkali, W., 1995, *Proc. ECOC*, Brussels, pp. 127–129.
[15] Yamaguchi, M., Matsunaga, T., Shirai, S., and Yukimatsu, K., 1994, *IECE Trans. Commun.*, **77,** 163.
[16] Zhuang, Z., Suh, S., and Patel, J. S., 1999, *Opt. Lett.*, **24,** 694.
[17] Hirabayashi, K., Tsuda, H., and Kurokawa, T., 1993, *J. Laser Technol.*, **11,** 2033.
[18] Ye, P., and Gu, C., 1999, *Optics of Liquid Crystal Displays* (Wiley).
[19] Lu, K., and Saleh, B. E., 1991, *Appl. Opt.*, **26,** 2354.
[20] Pain, F., Coquillé, R., Vinouze, B., Wolffer, N., and Gravey, P., 1997, *Opt. Commun.*, **139,** 199.
[21] Berreman, D. W., and Heffner, W. R., 1981, *J. appl. Phys.*, **52,** 3032.
[22] Guo, J., and Kwok, H., 2000, *J. appl. Phys.*, **39,** 1210.
[23] Dozov, I., Martinot Lagarde, P., Polossat, E., Lelidis, I., Giocondo, M., and Durand, G., 1999, *Proc. SPIE*, **3015,** 61.
[24] Meyer, R. B., 1977, *Mol. Cryst Liq. Cryst.*, **40,** 33.
[25] Lagerwall, S. T., 1999, *Ferroelectric and Antiferroelectric Liquid Crystals* (Wiley-VCH).
[26] Dupont, L., Glogarova, M., Marcerou, J. P., Nguyen, H. T., Destrade, C., and Lejcek, L., 1991, *J. Phys II*, **1,** 831.
[27] Walba, D., Dyer, D. J., Shao, R., Clark, N. A., Kundakila More, R. T., Thurnes, W. N., and Wand, M. D., 1993, *Ferroelectrics*, **148,** 435.
[28] Redmond, M., Coles, H., Wisherhoff, E., and Zentel, R., 1993, *Ferroelectrics*, **148,** 323.
[29] Sneh, A., Liu, J. Y., and Johnson, K. M., 1994, *Opt. Lett.*, **19,** 305.
[30] Sneh, A., and Johnson, K. M., 1995, *IEEE Photon. Technol. Lett.*, **7,** 379.
[31] Clark, N., and Lagerwall, S. T., 1980, *Appl. Phys. Lett.*, **36,** 899.
[32] Handschy, M. A., Johnson, K. M., and Moddel, G., 1988, *Ferroelectrics*, **85,** 279.

[33] KILLINGER, M., DE BOUGRENET DE LA TOCNAYE, J. L., CAMBON, P., CHITTICK, R. C., and CROSSLAND, W. A., 1992, *Appl. Opt.*, **31,** 333 930.
[34] MEARS, R. J., CROSSLAND, W., DAMES, M. P., COLLINGTON, J. R., PARKER, M. C., WARR, S. T., WILKINSON, T. D., and DAVEY, T., 1996, *IEEE JQE*, **2,** 35.
[35] BERTHELÉ, P., FRACASSO, B., and DE BOUGRENET DE LA TOCNAYE, J. L., 1998, *Appl. Opt.*, **37,** 5461.
[36] YAMAZAKI, H., and MATSUNAGA, T., 1998, *Ferroelectrics*, **231,** 225.
[37] BERESNEV, L. A., DULTZ, W., and HAASE, W., in Proceedings of conference on SLMs and their applications, Lake Tahoe, Spring 1996, pp. 174–176.
[38] PATEL, J. S., 1992, *Opt. Lett.*, **17,** 456.
[39] YIPTONG, A., MEARS, R. J., and PARKER, M. C., 1999, *Proc. Int. Photon. Res.*, RTuJ4.
[40] FUKUDA, A., TAKANISHI, Y., ISOZAKI, T., ISHIKAWA, K., and TAKEZOE, H., 1994, *J. mater. Chem.*, **4,** 997.
[41] VERHULST, A. G., CNOSSEN, G., FÜNFSCHILLING, J., and SCHADT, M., 1996, *Ferroelectrics*, **179,** 141.
[42] MEYER, B., 1969, *Phys. Rev. Lett.*, **22,** 918.
[43] BARBERI, R., GIOCONDO, M., and DURAND, G., 1992, *J. appl. Phys. Lett.*, **60,** 1085.
[44] PERTUIS, V., and PATEL, J. S., 1993, *Ferroelectrics*, **149,** 193.
[45] GUÉNA, M., LE GALL, M., DUPONT, L., and DE BOUGRENET DE LA TOCNAYE, J. L., 1998, *Ferroelectrics*, **213,** 439.
[46] CATANESCU, C. O., CHIEN, L.-C., and WU, S.-T., 2002, in Proceedings of ILC Conference, Edinburgh, June 2002, pp. 478–482.
[47] CLARK, N., and RIEKER, T. P., 1988, *Phys. Rev. A*, **37,** 1053.
[48] KHOO, I. C., 1994, *Liquid Crystals: Physical Properties and Nonlinear Optical Phenomena* (New York: Wiley).
[49] KHOO, I. C., CHEN, P. H., SHIH, M. Y., SHISHIDO, A., and SLUSARENKO, S., 2001, *Mol. Cryst. liq. Cryst.*, **358,** 1.
[50] DOANE, J. W., 1993, Bahadur ed., *Liquid Crystals Applications and Uses*, Vol. 1, edited by Bahadur (World Scientific), pp. 361–395.
[51] FERGASON, J. L., US patent 4 435 047.
[52] KITZEROW, H. S., 1996, in *Liquid Crystals in Complex Geometries*, edited by G. Crawford and S. Zumer (Taylor & Francis), Chap. 8.
[53] ZUMER, S., and DOANE, J. W., 1986, *Phys. Rev. A*, **34,** 3373.
[54] CROOKER, P. P., and YANG, D. K., 1990, *Appl. Phys. Lett.*, **57,** 2529.
[55] YAMAGUSHI, WAKI, and SATO, 1997, *Jpn. J. appl. Phys.*, **36,** 2771.
[56] TAKIZAMA, K., KODAMA, K., and KISHI, K., 1998, *Appl. Opt.*, **37,** 3181.
[57] RAMANITRA, H., CHANCLOU, P., VINOUZE, B., and DUPONT, L., 2002, *Electron. Lett.*, **38,** 1122.
[58] LOUKINA, T., CHEVALLIER, R., DE BOUGRENET DE LA TOCNAYE, J. L., and BARGE, M., 2003, *J. Laser Technol.*, **21,** 2067.
[59] MATSUMOTO, S., HOULBERT, M., HAYASHI, T., and KUBODERA, K., 1996, *Appl. Phys. Lett.*, **69,** 1044.
[60] MATSUMOTO, S., SUGIYAMA, Y., SAKATA, S., and HAYASHI, T., 1999, *J. intell. Mater. Syst. Struct.*, **10,** 489.
[61] MATSUMOTO, S., HIRABAYASHI, H., SAKATA, S., and HAYASHI, T., 1999, *IEEE Photon. Technol. Lett.*, **11,** 441.
[62] SHINSUKE, M., 2001, NTT, patent JP 2000 193 920.
[63] MOLSEN, H., and KITZEROV, H. S., 1994, *J. appl. Phys.*, **75,** 710.
[64] LUCCHETA, D. E., KARAPINAR, R., MANNI, A., and SIMONI, F., 2002, *J. appl. Phys*, **91,** 6060.
[65] SUTHERLAND, R. L., TONDIGLIA, V. P., and NATARAJAN, L. V., 1994, *Appl. Phys. Lett.*, **64,** 1074.
[66] DOMASH, L. H., CHEN, Y. M., HAUGSJAA, P., and OREN, M., 1997, *LEOS 97*, pp. 34–35.
[67] YERALAN, S., GUNTHER, J., RITUMS, D. L., CID, R., and POPOVICH, M., 2002, *Optical Engineering*, **41,** 1774.
[68] SUTHERLAND, R. L., 2002, *J. Opt. Soc. Am. B*, **19,** 2995.
[69] CAPUTO, R., SUKHO, A. V., TABIRYAN, N. V., ETON, C. U., and USHAKOV, R. F., 2001, *Mol. Cryst. liq. Cryst.*, **372,** 263.
[70] MACH, P., WILTZIUS, P., MEGENS, M., WEITZ, D., LIN, K. H., LUBENSKY, T., and YODH, A., 2002, *Europhys. Lett.*, **58,** 679.
[71] BOWLEY, C. C., FONTECCHIO, A. K., LIN, J. J., YUAN, H., and CRAWFORD, G., 1999, *Proc. mater. res. soc.*, Liquid Crystals, Materials and Devices, **559**, 97.
[72] BUNNING, T. J., NATARAJAN, L. V., TONDIGLIA, V. P., and SUTHERLAND, R. L., 1998, *Mol. Cryst.*, **30,** 127.
[73] ARCHAMBAULT, J. L., RUSSELL, S. J., BARCELOS, S., HUA, P., and REEKIE, L., 1994, *Opt. Lett.*, **19,** 180.
[74] HIKMET, R. A., 1991, *Liq. Cryst.*, **9,** 405.
[75] BOWLEY, C. C., ZUMER, S., and CRAWFORD, G. P., 1999, *SID Dig*. 32.
[76] FURUE, H., IMURA, Y., HASEBE, H., TAKATSU, H., and KOBAYASHI, S., 1998, *Mol. Cryst. liq. Cryst.*, **317,** 259.
[77] GAUTIER, P., BRUNET, M., GRUPP, J., SAUVAJOL, J. L., and ANGLARET, E., 2000, *Phys. Rev. E*, **62,** 7528.
[78] GUYMON, C. A., SHAO, R., DOUGAN, L. A., CLARK, N. A., HOELTER, D., FREY, H., and BOWMAN, C. N., 1998, *Liq. Cryst.*, **24,** 263.
[79] ADAMS, J., HAAS, W., and DAILEY, J., 1971, *J. appl. Phys.*, **42,** 4096.
[80] FUJIKAKE, H., KUKI, T., NOMOTO, T., TSUCHIYA, Y., and UTSUMI, Y., 2001, *J. appl. Phys.*, **89,** 5295.
[81] WU, H. G., ERDMANN, J. H., and DOANE, J. W., 1989, *Liq. Cryst.*, **5,** 1453.
[82] HIKMET, R. A. M., 1990, *J. appl. Phys.*, **68,** 4406.
[83] YAMAMOTO, S., EBIHARA, T., KATO, N., and HOSHI, H., 1991, *Ferroelectrics*, **114,** 81.
[84] JOHANSSON, M., HARD, S., ROBERTSON, B., MANOLIS, I., WILKINSON, T., and CROSSLAND, W., 2002, *Appl. Opt.*, **41,** 4904.
[85] WU, S. T., and LIM, K. G., 1987, *Appl. Opt.*, **26,** 1722.
[86] LEE, W. Y., LIN, J. S., and WANG, S. Y., 1995, *J. Laser Technol.*, **13,** 49.
[87] RANALLI, A. R., BRADLEY, A. S., and KONDIS, J. P., 1999, in Proceedings of ECOC'99, Nice 1999, pp. 68–69.
[88] PAIN, F., COQUILLÉ, R., VINOUZE, B., WOLFFER, N., and GRAVEY, P., 1998, in Proceedings of ECOC'98, Madrid 1998, pp. 295–296.
[89] CHIAO, J. C., 2001, *SPIE ITCom*, Denver August 2001, pp. 25–33.

[90] Fracasso, B., de Bougrenet de La Tocnaye, J. L., Razzak, M., and Uche, C., 2003, *J. Laser Technol.*, **21,** 2405.
[91] Parker, M. C., Cohen, A., and Mears, R., 1998, *J. Laser Technol.*, **16,** 1259.
[92] Penninckx, D., Khalfallah, S., and Brosson, P., 2001, *Proc. OFC 2001*, ThB4-1.
[93] Montgomery, G. P., 1989, *Proc. SPIE*, **1080,** 242.
[94] Wu, S. T., and Wu, C. S., 1991, *Mol. Cryst. liq. Cryst.*, **207,** 1.
[95] Tan, A., Bakoba, A., Wolffer, N., Vinouze, B., and Gravey, P., 2000, *Proc. SPIE*, **4089,** 208.
[96] Stinson, T. W., and Lister, J. D., 1970, *Phys. Rev. Lett.*, **25,** 503.
[97] F. Hoffman Laroche Inc., Basel.
[98] Jacobs, S. D., Cerquan, K. A., Marshall, K. L., Schmid, A., Guardalben, M. J., and Skerrett, K. J., 1988, *J. Opt. Soc. Am B*, **5,** 1962.
[99] Webb, J. E., 2001, *Proc. OFC 2001*, ThB1-1.
[100] Eldada, L., 2001, *Opt. Eng.*, **40,** 1165.
[101] Chiba, T., Ohtera, Y., and Kawakami, S., 1990, *J. Laser Technol.*, **17,** 885.
[102] Dupont, L., Le Gall, M., de Bougrenet de La Tocnaye, J. L., and Penninckx, D., 2000, *Opt. Commun.*, **176,** 113.
[103] Hinz, S., Sandel, D., Yoshida-Dierolf, M., Mirvoda, V., Noé, R., Weyrauch, T., and Haase, W., 2000, *Proceedings of the 7th International Conference on FLC*, Darmstadt, pp. 124–125.
[104] Dupont, L., Sansoni, T., and de Bougrenet de La Tocnaye, J. L., 2002, *Opt. Commun.*, **209,** 101.
[105] Achaya, B. R., Möller, L., Baldwin, K., MacHarrie, R., Huang, C., Pindak, R., and Rogers, R., 2002, in Proceedings of ECOC conference, Copenhagen, September 2002, PD2.8.
[106] Kobayashi, M., Terui, H., Kawachi, M., and Noda, J., 1982, *IEEE J. quantum Electron.*, **18,** 1603.
[107] Mitsuishi, M., Ito, S., Yamamoto, M., Fischer, T., and Knoll, W., 1997, *Liq. Cryst.*, **14,** 381.
[108] Evans, T., Reconfigurable transverse waveguide gratings for optical routing and wavelength manipulation, Cambridge Eng. Dept, Photonics Sensor Group report, 2002.
[109] Wong, C. S., Liu, J. Y., and Johnson, K. M., 1996, *Ferroelectrics*, **181,** 61.
[110] Gros, E., de Bougrenet de La Tocnaye, J. L., Coquillé, R., and Wolffer, N., 2000, *Ann. Telecommun.*, **55,** 342.
[111] Gros, E., and Dupont, L., 2001, *IEEE Photon. tech. Lett.*, **13,** 115.
[112] Binet, C., Mitov, M., and Mauzac, M., 2001, *J. appl. Phys.*, **90,** 1730.
[113] De Vries, H., 1951, *Acta Crystallogr.*, **4,** 219.
[114] Yip, W. C., Huang, H. C., and Kwok, H. S., 1997, *Appl. Opt.*, **36,** 6453.
[115] De Bougrenet de La Tocnaye, J. L., and Dupont, L, 1998, *Appl. Opt.*, **36,** 1730.
[116] Johnson, K. M., McKnight, D. J., and Underwood, I., 1993, *IEEE J. quant. Electron.*, **29,** 699.
[117] Crossland, W., Manolis, I. G., Redmond, M., Tan, K. L., Wilkinson, T., Holmes, M. J., Parker, T. R., Chu, H., Croucher, J., Handerek, V. A., Warr, S. T., Robertson, B., Bonas, I., Franklin, R, Stace, C., White, H. J., Woodley, R. A., and Henshall, G., 2000, *J. Laser Technol.*, **18,** 1845.
[118] Dupont, L., and de Bougrenet de La Tocnaye, J. L., 1997, *Opt. Commun.*, **142,** 208.
[119] Gravey, P., de Bougrenet de La Tocnaye, J. L., Fracasso, B., Wolffer, N., Tan, A., Vinouze, B., and Razzak, M., 2003, *Ann Telecommun.*, **58,** 38.
[120] Sinzinger, S., and Testorf, M., 1995, *Appl. Opt.*, **34,** 5970.
[121] Wand, X., Wilson, D., Muller, R., Maker, P., and Psaltis, D., 2000, *Appl. Opt.*, **39,** 6545.
[122] http://www.jvc-victor.co.jp/english/pro/dila/device.html
[123] http://www.crlopto.com/products/index.php
[124] De Bougrenet de La Tocnaye, J. L., 2000, *Liquid Crystal-based Optical Space Switches for DWDM Networks*, Proc. Flcmrc meeting (http://flcmrc.colorado.edu/telecom_downloads.html), Boulder, June 2000.
[125] Oh, M. C., Lee, H. J., Lee, M. H., Ahn, J. H., Han, S. G., and Kim, H. G., 1996, *Appl. Phys. Lett.*, **73,** 1190.
[126] Yariv, A., and Nakamura, M., 1977, *IEEE J. quantum Electron.*, **13,** 233.
[127] Sirleto, L., Coppola, G., Abbate, G., Righini, G., and Oton, J. M., 2002, *Opt. Eng.*, **41,** 2890.
[128] Veilleux, C., Lapierre, J., and Bures, J., 1986, *Opt. Lett.*, **11,** 733.
[129] Verbrugge, V., de Bougrenet de La Tocnaye, J.-L., and Dupont, L., 2002, *Opt. Commun.*, **215,** 353.
[130] Vakhshoori, D., Tayebati, T., Cheng, C., Azimi, M., Wang, P., Zhou, J. H., and Canoglu, E., 1999, *Electron. Lett.*, **35,** 900.